NUCLEAR FISSION AND
RADIATION PROTECTION

SEVENTH FRAMEWORK
PROGRAMME

Passive and Active Systems on Severe Accident source term Mitigation (PASSAM project)

PASSAM-DKS-T28 [D5.5]
IRSN/PSN-RES/SEREX/2017- 00165
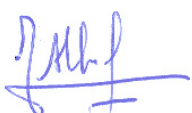
PASSAM Final Synthesis Report

T. Albiol (IRSN), L. Herranz (CIEMAT), E. Riera (CSIC), C. Dalibart (EDF),
T. Lind (PSI), A. Del Corno (RSE), T. Kärkelä (VTT), N. Losch (AREVA),
B. Azambre (UniLor), C. Mun (IRSN), L. Cantrel (IRSN)

Period covered: January 2013 – December 2016	Delivery date: February 2017	
Start date of PASSAM: January 1st, 2013	Duration: 4 years	
WP N°5	WP leader: T. Albiol	WP Leader's organization: IRSN

PASSAM Quality Assurance page

Partner responsible of the document: IRSN			
Type	Progress and Technical Document		
Reference(s)	PASSAM–DKS-T28 [D5.5] IRSN/PSN-RES/SEREX/2017 – 00165		
Title	PASSAM Final Synthesis Report		
Author(s)	T. Albiol (IRSN), L. Herranz (CIEMAT), E. Riera (CSIC), C. Dalibart (EDF), T. Lind (PSI), A. Del Corno (RSE), T. Kärkelä (VTT), N. Losch (AREVA), B. Azambre (UniLor), C. Mun (IRSN), L. Cantrel (IRSN)		
Delivery date	February 2017		
Revisions	Revision 1	Date: /	Main modifications
WP	WP N°5, DKS		
For Journal & Conf. papers	J or C. reference:		
	Related Web site:		

Summary

This report constitutes the technical part of the final synthesis report of the European PASSAM project. After a short presentation of the context and objectives of the Project, it provides a synthesis of the major results obtained by the nine partners of this four year project.

A full page executive summary is provided in page 8.

Visa grid			
	Main author(s)	Verification	Approval
Names	T. Albiol	Management Team members (by email)	Steering Committee members (by email)
Date	February 23rd, 2017	February 23rd, 2017	February 23rd, 2017
Signatures		/	B. Chaumont, Steering Committee Chairman

IRSN

INSTITUT
DE RADIOPROTECTION
ET DE SÛRETÉ NUCLÉAIRE

Enhancing nuclear safety

PASSAM Final Synthesis Report

T. Albiol (IRSN), L. Herranz (CIEMAT), E. Riera (CSIC),
C. Dalibart (EDF), T. Lind (PSI), A. Del Corno (RSE),
T Kärkelä (VTT), N. Losch (AREVA), B. Azambre
(UniLor), C. Mun (IRSN), L. Cantrel (IRSN)

Pôle sûreté des installations et des systèmes nucléaires
Service d'Étude et de Recherche Expérimentale

PASSAM Final Synthesis Report
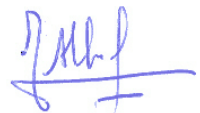
IRSN/PSN-RES/SEREX/2017- 00165
PASSAM-DKS-T28 [D5.5]

	Rédacteur(s) *Author(s)*	Vérificateur(s) *Reviewer(s)*	Chef d'unité *Head of unit*	Chef de service *Head of department*	Directeur *Director*
Nom *Name*	T. Albiol et al	MT members (by e-mail)	/	M. Petit	p.o. B. Chaumont
Date	February 23rd, 2017	February 23rd, 2017	/	February 23rd, 2017	February 23rd, 2017
Visa					

Qualité
Quality

Nom *name*	C. Donque-Gomez
Date	February 23rd, 2017
Visa	

Projet
Project

Nom *name*	T. Albiol
Date	February 23rd, 2017
Visa	

![IRSN logo] INSTITUT DE RADIOPROTECTION ET DE SÛRETÉ NUCLÉAIRE

Fiche descriptive du rapport
Report description sheet

Titre

Sous-titre

Title: PASSAM Final Synthesis Report

Sub title

Auteur/author(s) : T. Albiol (IRSN), L. Herranz (CIEMAT), E. Riera (CSIC), C. Dalibart (EDF), T. Lind (PSI), A. Del Corno (RSE), T. Kärkelä (VTT), N. Losch (AREVA), B. Azambre (UniLor), C. Mun (IRSN), L. Cantrel (IRSN)

Type de document : *Document type :*		Date de diffusion : *Distribution date :*	**February 2017**
Référence PLEIADE:	**PSN-RES/SEREX/2017 – 00165**	**E-mail de l'auteur :**	**thierry.albiol@irsn.fr**
Références complémentaires	☐ BDD-ST n°: ☒ Programme n°: PASSAM-DKS-T28 [D5.5] ☐ Affaire n°:		
Elément DPPA	**1.9.1.4 – Affaire budgétaire : 30000583**		

Mots-clés (Max. 5) :	
Key-words (Max. 5):	**PASSAM – FCVS – Mitigation – severe accident**

RÉSUME

ABSTRACT

This report constitutes the technical part of the final synthesis report of the European PASSAM project. After a short presentation of the context and objectives of the project, it provides a synthesis of the major results obtained by the nine partners of this four year project.

A full page executive summary is provided on page 8.

IRSN

Content

List of tables

List of figures

1 Executive summary

The PASSAM (Passive and Active Systems on Severe Accident source term Mitigation) project was launched in the frame of the 7th framework programme of the European Commission. Coordinated by IRSN, this four year project (2013 – 2016) involved nine partners from six countries: IRSN, EDF and University of Lorraine (France); CIEMAT and CSIC (Spain); PSI (Switzerland); RSE (Italy); VTT (Finland) and AREVA GmbH (Germany).

It was mainly of an R&D experimental nature and aimed at investigating phenomena that might enhance atmospheric source term mitigation in case of a severe accident in a Nuclear Power Plant (NPP), mainly through the use of Filtered Containment Venting Systems (FCVS). Both already existing systems (i.e., water scrubbing and sand bed filters plus metallic pre-filters) and innovative ones (i.e., acoustic agglomerators, high pressure sprays, electrostatic precipitators, advanced zeolites and combined wet-dry filtration systems), were experimentally studied in conditions as close as possible to those anticipated for severe accidents. The objective consisted of exploring potential enhancement of existing source term mitigation devices and demonstrating the ability of innovative systems to achieve even larger source term attenuation.

Pool scrubbing represented the most studied domain of the PASSAM project. As an example of results, it was shown that gas hydrodynamics, at least in some relevant scenarios, is significantly different from what is nowadays encapsulated in severe accident analysis codes, particularly at high velocities and, that in the long run, maintaining an alkaline pH in the scrubber solution is absolutely necessary for preventing a delayed iodine release.

Regarding sand bed filters plus metallic pre-filters, implemented on all French nuclear power plants, filtration efficiency for gaseous molecular and organic iodine was checked. Other experiments, still in the PASSAM frame, showed that under severe accident conditions, cesium iodide aerosols trapped in the sand filter are unstable and may constitute a delayed source term, which is not the case for CsI particles trapped on the metallic pre-filter.

As innovative processes, both acoustic agglomeration and high pressure spray systems were studied mainly in the aim of leading to bigger particles upstream of filtered containment venting systems (FCVS), and so enhancing the filtration efficiency. An increase of the particle size by ultrasonic fields was experimentally observed and, as a secondary effect, aerosol mass concentration was decreased. As for high pressure spray, the increase in particle size could not be really measured, but the system showed a good efficiency: it allowed reducing the airborne particle concentration much more efficiently than low pressure sprays.

Experimental studies for trapping gaseous molecular and organic iodine using wet electrostatic precipitators (WESP) confirmed the importance of optimizing the WESP design and the usefulness of different process steps (e.g. oxidation of I_2 or CH_3I into iodine oxide particles) for a good trapping efficiency. The influence of several parameters, such as steam content, was also studied.

Extensive testing of zeolites as regards their capability for trapping gaseous molecular and organic iodine was performed, showing very good trapping efficiencies. Pre-selected zeolites were compared in various conditions: silver Faujasite-Y zeolite gave the best results. The global stability of trapped iodine under irradiation and steam conditions has also been checked.

The combination of a wet scrubber followed by a zeolite filtration stage was studied in representative severe accident conditions and showed its ability to reach a very good retention for gaseous organic iodides.

The project's outcomes constitute a valuable database which may be strategic for helping the utilities on the decision of implementing and/or enhancing mitigation systems on their reactors and for improving severe accident management, as well as helping regulators for improved assessment of the source term mitigation by different systems.

Simple models and/or correlations result from in-depth analysis of most of PASSAM experimental results. Once implemented in accident analysis codes, like ASTEC, these models should allow enhancing the capability of modelling Severe Accident Management scenarios and developing improved guidelines.

2   Summary description of project context and objectives

After the TEPCO Fukushima accident of March 2011, one of the main concerns of the nuclear industry has been the search for improved atmospheric source term mitigation systems. The motivation underneath stems from two major evidences: venting of the containment building might be an essential accident management measure in order to prevent the loss of its mechanical integrity, but this containment venting might result in substantial radioactive releases if no efficient source term mitigation system is implemented.

Some countries like Sweden, Switzerland, Finland, Germany and France, had already implemented Filtered Containment Venting Systems (FCVS) in the early 1990's as a mean to enhance their Nuclear Power Plants (NPPs) safety. The Netherlands, China and Bulgaria followed before the Fukushima accident. Many other countries have considered (and several of them decided) the implementation of FCVS more recently, in the post-Fukushima context.

This renewed interest for FCVS has pushed new national R&D programmes on this topic in several countries and new coordinated international activities, like writing a status report by the working group on the Analysis and Management of Accidents of the CSNI (Committee on the Safety of Nuclear Installations) of the OECD-NEA [1], or launching the European Commission (EC) project on "Passive and Active Systems on Severe Accident source term Mitigation" (PASSAM).

The industrial FCVS are essentially based on two approaches: "dry" and "wet" systems. In dry systems, large trapping surfaces are provided either by gravel or sand beds, or by metal fibers or by molecular sieves. In wet systems, trapping occurs in a liquid (water plus additives) pool as a consequence of several removal mechanisms the efficiency of which depends strongly on thermal-hydraulic conditions. These systems can be enhanced by including venturi scrubbers: water droplets injected into the gas stream capture aerosol particles and make them more easily trapped by subsequent filter systems.

In 2012, when launching the PASSAM programme, these systems, some of which were installed on NPPs, had been well characterized as regards aerosol retention efficiency, but to a far lesser extent as regards volatile iodine retention, including organic iodides. Indeed, more recent tests had been performed on FCVS for trying to improve the systems as regards organic iodides retention in water pools. Nevertheless the research on this specific aspect needed to be complemented. A lack of knowledge also appeared clearly for organic iodine retention in dry systems.

In parallel, several alternative and innovative approaches were appearing in the literature or are even already proposed by some vendors. Electric filtration systems were already widely used for many decades for many industrial applications, out of the nuclear field. Solutions based on molecular sieves (improved zeolites, metal organic frameworks, etc…) were also widely used as filter in many industrial processes. Many kinds of zeolite exist; a key point consisted of finding the most efficient zeolite for iodine species in severe accident conditions. Another promising innovative solution relied on the combination of wet and dry filter systems. Besides, as it is well known that, generally speaking, the filtration systems are less efficient for aerosol particles of some tenths of microns, some systems were being developed, aiming at agglomerating aerosol particles in order to get bigger particles which would be better filtered (acoustic systems, high pressure sprays ...). Implementing such a device upstream of a filtration system could overcome the decrease of filtration efficiency of sub-micron particles.

Another subject which had been studied to only limited extent is the stability of the trapped fission products on the medium and long term (up to some days) following a nuclear accident. Indeed, the trapped fission products may be re-vaporized and/or re-entrained due to surrounding conditions relevant to an accident and more especially, due to continuous irradiation, coupled to continuous flow-rate (if the venting system remains open), and to high temperature and humidity. Indeed the re-entrainment of trapped aerosols was tested in different small scale facilities and, at larger scale, in the international ACE programme [2] where the filters loaded with aerosol (dry and wet filters) were operated with clean gas and the aerosol concentrations of the gas downstream of the filters were measured. Nevertheless, no data on delayed release, under typical FCVS conditions (including irradiation) both for trapped aerosols and gaseous iodine forms, could be found in the open literature.

In this context, the PASSAM project has been built to explore potential enhancements of existing source term mitigation devices and check the ability of innovative systems to achieve even larger source term

attenuation. Heavily relying on experiments, the PASSAM project aimed at providing new data on the capability and reliability of a number of systems related to FCVS: pool scrubbing systems, sand bed filters plus metallic prefilters, acoustic agglomerators, high pressure sprays, electrostatic precipitators, improved zeolites and combination of wet and dry systems. Nonetheless, the scope of some of the PASSAM research topics - as fission products and aerosol retention in water ponds - goes beyond FCVS and might be applied to accident situation other than containment venting, e.g. for fission product scrubbing in the suppression pool of a Boiling Water reactor (BWR) or in the secondary side of a steam generator during a Steam Generator Tube Rupture (SGTR) accident if the secondary side is flooded.

Besides an extension of the existing experimental database on existing and innovative filtration systems, the focus was put on trying to get a deeper understanding of the phenomena underlying their performance and to develop models/correlations that allow modelling of the systems in accident analysis codes, like ASTEC [3].

The PASSAM project was launched under the 7th framework programme of EURATOM for four years, formally from January 2013 to December 2016, and practically up to March 2017. Gathering 9 organizations (IRSN, EdF and University of Lorraine, France; CIEMAT and CSIC, Spain; PSI, Switzerland; RSE, Italy; VTT, Finland; and AREVA GmbH, Germany) and coordinated by IRSN, the project involved about 400 person-months and the associated cost was more than 5 M€.

The planning of the PASSAM project was rather linear as a whole, with three conceptual phases:
- set-up of organizational bases and of experimental facilities (2013);
- execution of experimental campaigns (mid 2013 to end 2016);
- in depth analysis of the experimental results and project wrap-up (mid 2015 to early 2017).

The first phase included a literature survey on the existing and innovative systems to be experimentally studied in the project [4]. This survey confirmed, with more details, the anticipated gaps of knowledge and hence allowed optimizing the test matrices for each experimental work-package [5]. It ended up with an open workshop held in Madrid (Spain) in February 2014 [6].

The experimental studies, which constitute the largest part of the PASSAM activities, are described in the next section of this paper together with the rationale for exploring each of the studied systems and a selection of some of the major results.

The last phase of PASSAM consisted mainly of two points. An in-depth analysis of the experimental results allowed developing models and/or correlations based on the experimental results. The corresponding outcomes are presented together with the experimental results in the next section of this report.

In parallel, the project outputs were managed in the best way so that nuclear community can easily benefit from the research conducted:
- a final PASSAM workshop was organized on February 28th and March 1st, 2017 in Paris (France),
- the present final synthesis report of the project is made available in open literature,
- forty-three (43) PASSAM papers were issued in scientific journals and conferences by the PASSAM partners.

3 Description of main S&T results/foregrounds

3.1 Experimental Studies of Pool Scrubbing Systems

Removal of contaminating particles and/or vapours from a carrier gas, when passing through an aqueous pond, is known as pool scrubbing. Most pool scrubbing investigation dates back to 1980's and 1990's [7].

In the last 20 years, there have been a few specific studies focused on hot pools [8] and jet regime [9]. These experimental campaigns, however, were limited in their scope. More recently, some additional information on pool scrubbing of aerosols has been gained through the ARTIST projects [10, 11], in which the most distinctive element was the presence of submerged surfaces representing the secondary side of a steam generator.

The gathered database allowed drawing some insights into pool scrubbing but there are still significant weaknesses: lack of systematic analysis of the parameters influencing pool scrubbing (i.e., submergence, particle size, steam content, etc.); no experimental tracking of variables like bubble size and shape; conditions hardly addressed in the past, such as jet injection or in-pool gas rise under churn-turbulent regime; few experiments on scrubbing of fission products vapors. No less important, since the experimental programs were performed, some know-how has been lost throughout the years.

There are a good number of studies concerning bubble hydrodynamics out of the nuclear safety community. However, they mostly address conditions far from those anticipated in severe accidents. Anyway, the existing significant information was taken into account in the analysis of the results and modelling phases.

The PASSAM pool-scrubbing work-package is, by far, the biggest one of the PASSAM project, which is consistent with the above statements and with the wide use of pool scrubbing systems as FCVS in many NPPs. Five main topics were studied. A specific paper on the status of these studies was presented at an IAEA conference in September 2015 [12]. Now, at the end of the PASSAM project, the main outcomes resulting from these studies can be synthesized as presented in the following sub-sections.

3.1.1 Pool scrubbing under jet injection regime

A series of tests were performed in the CIEMAT PECA facility (hereafter, PSP campaign), focusing on aerosol retention at the nearby of the injection point under high gas velocities (i.e., the jet injection regime). Two major boundary conditions of retention at the inlet of the pool were considered: the gas mass flow rates (i.e., gas injection velocity) and the saturation state of the pool. The former was controlled through the non-dimensional Weber number (i.e., ratio between inertia and surface tension forces) and the latter through the gas saturation ratio (i.e., ratio between steam pressure in the carrier gas and saturation pressure at the pool temperature). Through this approach the role that thermal-dependent mechanisms (i.e., diffusiophoresis) and "entrained-droplet mechanisms" (i.e., inertial impaction and interception) play in the "near-field" retention was assessed. Table 1 shows the experimental matrix of the PSP campaign. The submergence was set to 0.3 m in all the tests and the same particles were used all across the test matrix: 1 μm SiO_2.

Table 1: PSP experimental test matrix

Test	T_{gas}(°C)	T_{pool}(°C)	Q_{steam}(l/min)	Q_{total}(l/min)	X_{steam}(%$_{vol}$)	We	S
PSP0	100	35	5	160	3.13	2.36E+05	0.59
PSP1	100	35	6	210	2.86	1.02E+06	0.56
PSP2	100	35	9	310	2.9	2.21E+06	0.61
PSP3	100	35	15	460	3.26	4.87E+06	0.79
PSP4	100	35	30	460	6.52	4.87E+06	1.57
PSP5	100	35	45	460	9.78	4.87E+06	2.36
PSP6	T_{env}	T_{env}	0	460	0	4.87E+06	0

The reduced submergence was set to preclude the bubble swarm rise region as much as possible. The air-steam mixture was injected at flow rates ranging from 150 to 450 l/min via a single-hole horizontal injector. Note that We was in all the tests over the jet regime threshold (10^5) and the explored range of S allowed both condensing (S>1.0) and evaporating conditions (S<1.0).

Some visual observations of the hydrodynamics were made. The hydrodynamic characteristics which potentially affected the pool retention capability were: (i) jet injection occurred in a pulsated way, which frequency grew with gas flowrate (at the same pressure conditions at the injection point); (ii) the submerged jet trajectory was not steady and, once bending upwards, the location of the jet vertical axis oscillated; (iii) the transition from a quasi-horizontal jet to a fully developed bubble swarm region already started in the 30 cm water depth; (iv) the water surface was rough and wavy.

As for jet scrubbing, the volumetric flow rate played a major role in the pool absorption of the injected particulate matter (Figure 1). The growing trend observed when flow rates are increased from about 150 l/min to 300 l/min gets to a sort of asymptotic value around 97% at even higher flow rates. This is consistent with the fact that a high gas flow rate means a strong interaction in the gas-water interface (i.e., shear stress) that eventually causes water entrainment in the form of droplets within the gaseous bulk. Contrary to what was observed with gas flow rates, scrubbing efficiency was not apparently affected (at least not noticeably) by steam fraction and gas-pool temperature difference.
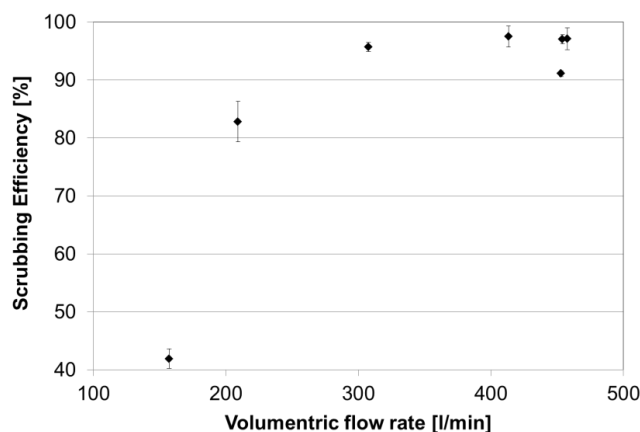
Figure 1: PSP scrubbing efficiency vs. volumetric flow rate.

The limited number of tests conducted is a strong shortcoming to derive any correlation from the data gathered. Nonetheless, it is worth exploring the dependencies for the retention efficiency (ε) that might be found according to the executed test matrix:

$$\varepsilon = f(We; S)$$

By setting a logarithmic dependence on We and a sort of linear on S, some promising form of correlations with R^2 over 0.80 have been found. This is still very premature and some more data should be used to consolidate both trends in a single equation.

In short, particle scrubbing at the pool inlet region is highly efficient once jet injection is well developed (i.e., We $\geq 10^6$, approximately), regardless of the thermal boundary conditions. Mechanical processes become responsible for a particulate mass removal higher than 90% once We $> 2 \cdot 10^6$; according to observations, inertial impaction is postulated to be the dominant aerosol removal mechanism. As for outlook, experimental investigation on jet injection scrubbing should be further continued to build a broad and reliable database supporting development and/or validation of suitable models; this experimentation should be associated to hydrodynamic tests aiming at characterizing features of the entrained droplets. Given the strong interaction among multiple phases in jet scrubbing (i.e., particulate matter, non-condensable gas, steam and water), the experimental work to be done should carefully watch out the scaling of the set-up and the boundary conditions.

3.1.2 Pool scrubbing and hydrodynamics in natural water, sea water and in the presence of additives

In the framework of pool scrubbing studies, two different experimental campaigns were carried out using the RSE SCRUPOS facility: one focused on hydrodynamic studies and the other one concerning aerosol retention. The tests were performed with different aerosol sizes (0.4, 1 μm), different sized nozzles (10, 20 and 50 mm), three mass flow rates and three different liquid compositions. During the hydrodynamic tests, measures on bubble size, aspect ratio, velocity and local void fraction were obtained using three technics (optical probe, photo camera and video camera).

The facility reproduces a small scale bare pool with dimensions 500x1000 mm with a height of 1500 mm with a single vertical nozzle. The liquid phase was either demineralized water, sea water (used in Fukushima) or water with surfactant (chosen to change significantly the surface tension). The tests on bubble hydrodynamics were performed with injection velocity from 3 to 74 m/s in order to have different flow regimes. For every test conditions, the optical probe measurements were taken at three distances from the nozzle (to intercept the bubbles in the injection zone, in the break up zone and in the rise zone) and at different radial distances from the centre of the gas flow in order to better monitor bubble behaviour making a map of bubble sizes and velocities.

The bubble dimensions obtained considering the peak of the local void distribution vs bubble chord calculated with optical probe measurements were confirmed by the image analysis (Figure 2 (a-b-c-d-e-f)). In a bare pool, the different injection flow rates and nozzles generated different initial bubble structures: bubble (Figure 2 (a -b)) and churn-turbulent (Figure 2 (d- e)) in the injection zone, but after only 20-30 cm, they were broken into typical bubbles of a bubble regime. In the injection zone the local void distribution vs bubble chord was a bimodal function. In fact, the gas flow was composed of large bubbles around 50-100 mm and small bubbles around 10-20 mm (Figure 2 (c-f)). After 20-30 cm, this bimodal distribution became a lognormal one with a peak at 4-8 mm (Figure 2 (g-h)). The sizes and velocities of the bubbles measured at 60-70 cm from the nozzle are similar regardless of the nozzle diameter and the mass flow rate, indicating that the flow was mainly controlled by buoyancy: the velocity was close to 0.8-1.2 m/s and bubbles size between 4.5-6 mm (depending on the velocity). Absolute bubble velocity was proportional to local void fraction. These bubble velocities were higher than those modelled in pool scrubbing codes.

In the tests with the three liquid compositions, in the bubble regime, the bubble size distributions and velocities were the same regardless of the water composition (Figure 2 (c)). In the jet regime and in the injection zone, the bubble size distributions in seawater and in water with surfactant were similar to each other but smaller than in pure water (Figure 2 (f)). The difference in globular formation size was due, in the case of the surfactant, to the higher tendency to break-up because of the lower surface tension and, for the seawater, to the inhibited coalescence due to the presence of electrolytes. On the other hand, Weber number on which the break up condition is based (We=$\geq 12\zeta$, where ζ is a function of the aspect ratio) for water and sea water were similar and twice that of water with surfactant. Near the nozzle (7cm), the bubble velocity for a mass flow rate of 18 kg/h in demineralized water was 5 m/s and in sea water and water with surfactant it was around 3.3 m/s: the difference was due to different bubble size distribution.

The local void fraction values in the closest region to the nozzle were from 26% to 57 % depending on gas injection velocity and nozzle size. When the large bubbles break, the swarm expands during the rising to the pool surface due to lift force that tends to move small bubbles towards the side of low liquid velocities, i.e. external side of the swarm [13]. At 60-70 cm from the nozzle the local void fraction was around 8-10% and 88% of the swarm was inside a zone of 20 cm diameter. At 80-90 cm from the nozzle there is not big variation on bubble swarm and it confirms that, at that position, the bubbles were in the rise zone (Figure 3).

The pool scrubbing tests with aerosols showed that the scrubbing efficiency (or rather the Decontamination Factor (DF) classically defined as the amount of a pollutant upstream divided by the amount of a pollutant downstream from a filtering device) increases almost by a factor of two when comparing the surfactant and the sea water to the demineralized water for 0.4 μm SiO_2 particles (Figure 4). This was due to an increased interfacial area between the liquid and the gas phase, and a different residence time in the pool. A higher DF for 1 μm than for 0.4 μm aerosol was also evidenced (Figure 4).

Bubble regime			Jet regime		
We= $3.9 \cdot 10^4{}_{water}$	We=$4 \cdot 10^4{}_{sea}$	We=$7.8 \cdot 10^4{}_{surf}$	We=$6.9 \cdot 10^5{}_{water}$	We=$7.1 \cdot 10^5{}_{sea}$	We=$13.9 \cdot 10^5{}_{surf}$
Demineralized water		Sea Water	Demineralized water		Water with surfactant

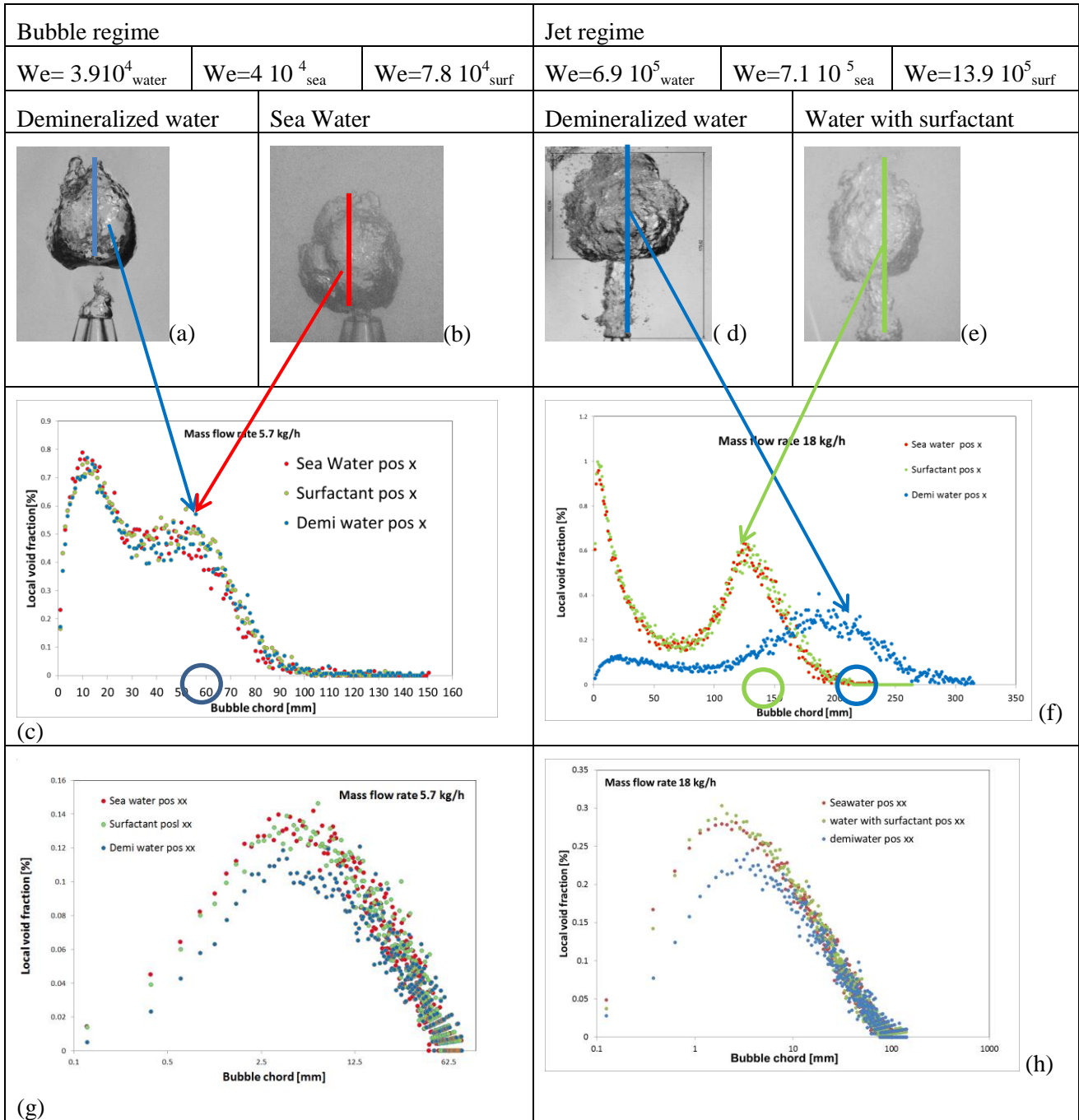Figure 2: Bubble images in the injection zone for mass flow rate of 5.7 kg/h in demineralized water (a) and sea water (b) and for mass flow rate 18 kg/h in water (d) and water with surfactant (e). Local void fraction distribution at 7.6 cm (pos x) and at 23 cm (pos xx) from the top of the 10 mm vertical nozzle, in central radial position in three different pool liquid for mass flow rate of 5.7 kg/h (c-g) and for 18 kg/h (f-h).
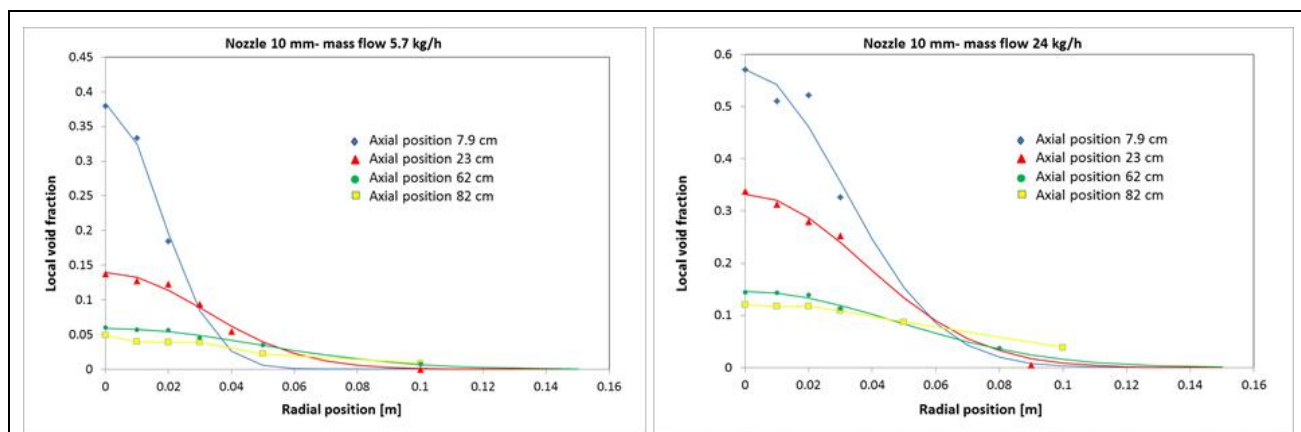
Figure 3: Local void fraction profiles in demineralized water with 10 mm injection nozzle at 5.7 kg/h and 24 kg/h mass flow rate.
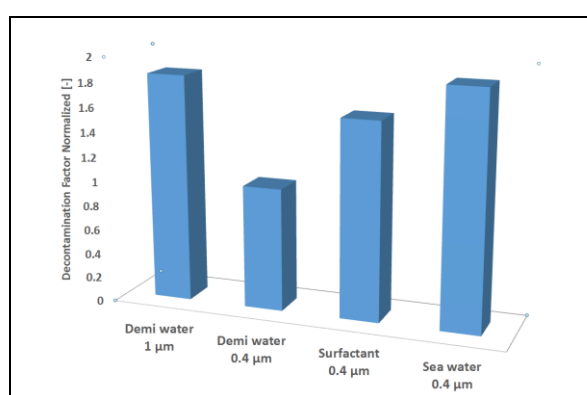
Figure 4: Decontamination Factor in demineralized water for a 0.4 and 1 μm SiO_2 aerosol and in sea water and water with surfactant for 0.4 μm SiO_2 aerosol normalized from DF in demineralized water for a 0.4 μm SiO_2 for a nozzle submergence of 1 m.

The tests allowed validating a simplified model to describe the evolution of the bubbles inside the pool and the decontamination. The model takes into account both the decontamination in the injection zone (DF_{jet}) due to the three phase liquid-gas-droplet model [14] where some decontamination models and parameters are obtained from Porcheron [**Erreur ! Source du renvoi introuvable.**] and from PASSAM experimental data [16], and a decontamination in the break-up and in the rise zones based on ECART and SPARC equations for bubble regime (DF_{rise}). In the model, the residence time is obtained considering an experimental absolute bubble velocity. Aerosol removal (DF_{rise}) is due to the mechanisms of gravity sedimentation, centrifugal impaction and Brownian diffusion. Centrifugal impaction depends on the internal gas velocity circulation that is not easily determined due to not spherical bubble shape and bubble relative velocity compared to the liquid phase velocity. For bubble size evolution, a bubble break-up rate is introduced [17] and it represents another sensitivity parameter.

The experimental data collected both on the hydrodynamics and bubble behaviour, and on aerosol decontamination for the same operative conditions allowed to collect an interesting data base for testing aerosol codes. The different behaviour in the liquid phases finally has confirmed that bubble fragmentation increases bubble surface and aerosol retention and so ad-hoc devices (obstacles, grids, etc.) should be used to improve the scrubbing efficiency.

3.1.3 Pool hydrodynamics under SGTR conditions

The ARTIST project showed that during a steam generator tube rupture (SGTR) with fission product release, the aerosol particle retention in the secondary side of the steam generator was significantly increased due to the presence of submerged structures, i.e., the tube bundle, as compared to a bare pool. The increased aerosol retention was attributed to the interactions of the high velocity gas jet discharged from the tube break

with the dense bundle of the steam generator tubes. To understand the aerosol transport in the steam generator secondary side, the hydrodynamic behaviour of the two-phase flow needs to be characterized. Under these conditions, the two-phase flow is expected to be very complex due to the high gas velocities and complicated geometry of the steam generator secondary side.

To investigate two-phase flow in the tube bundles, a hydrodynamic facility called TRISTAN (Tube Rupture In Steam generaTor: multi-phAse-flow iNvestigations) was designed and constructed at PSI. For comparison between a bare pool and a tube bundle, the design allows the use of a single tube or a tube bundle in the facility. The facility has a square cross-section of 500x500 mm and the height of 6 m. In these experiments, the facility was operated at ambient conditions.

A set of two wire-mesh sensors with 120x120 channels and a wire-pitch of 3.4 mm are used to measure the void fraction over the whole cross-sectional area of the facility with the frequency of 1024 Hz. In this work, the facility was equipped with a tube bundle consisting of 221 steam generator tubes, or with a single tube in the center of the facility. For the gas injection, two different break types were used, the "guillotine" and the "fish-mouth" break. The guillotine break represented a full circumferential breach of the steam generator tube whereas the fish-mouth break represented a diamond shaped breach of the tube. The break area in both geometries corresponded to the flow area in a steam generator tube of A=227 mm^2. The flow development was followed by measuring the void fraction at different distances from the gas injection point and using different flow rates. The bubbles which were too small to be detected with the wire-mesh sensor were measured using a high-speed camera and the image analysis method.

The measurements were carried out at four different distances between the injection point and the wire-mesh sensor, between 100 and 2500 mm, and at three different flow rates, namely 50, 250, and 450 kg/h. Void fraction, bubble size distributions, gas phase velocity as well as interfacial area concentration were determined based on the wire-mesh sensor data. In addition, the penetration depth of the initial large gas bubble into the channel was studied for the closest break-to-sensor distance.

The foremost observation of the flow hydrodynamics was the existence of very large volumes of gas with varying shapes, and the chaotic, dynamic behaviour of the flow, Figure 5. The tube bundle showed a significant confining effect to the spreading of the gas jet with less penetration depth than in the bare pool, Figure 6. Also, the gas volume given as the void fraction was laterally more concentrated close to the injection tube in the tube bundle than in the bare pool. The bubble size distributions were similar with the two set-ups showing a rather bimodal distribution with a large number of small bubbles with the spherical equivalent diameter of 5-10 mm and with a second peak at bubble diameters larger than 100 mm. Even though small in number, the large bubbles represented a considerable amount of the gas phase volume. The large bubble peak was more pronounced in the tube bundle than in the bare pool set-up showing the effect of the tube bundle on the preservation of the large continuous gas volumes which typically remained in the center of the flow area adjacent to the injection tube.

The interfacial area concentration is important to determine due to its critical function in defining the mass transfer from the gas bubbles to the liquid. Therefore, considerable efforts were made to determine the interfacial area concentration under the challenging flow conditions of the present work. The results show that with similar injection flow rates, the interfacial area concentration was higher in the tube bundle than in the bare pool, especially at higher gas flow rates. This was presumably due to the break-up of the bubbles in the tube bundle due to the interaction of the gas jet with the tubes.

This work on the hydrodynamics of the jet injection regimes has permitted valuable insights on the dominating fluid flow regimes. In particular, the detailed bubble size, shape, interfacial area and velocity data will allow more credible estimates of the multiphase phenomena than corresponding models in existing low injection regime codes. It can be argued that the decontamination factors in jet regimes by current aerosol pool scrubbing codes are reasonable only because of canceling errors. Indeed, the assumed small bubble diameters and corresponding high residence times combine to give large DF's. The TRISTAN jet injection hydrodynamic tests show that residence times are a lot shorter and the equilibrium bubble diameters a lot larger than assumed in the codes. Therefore, a thorough overhaul of modeling of jet injection phenomena is required, and a particular focus should be devoted to the phenomena very near the injection point.

Figure 5: Selected bubbles in the single tube set-up with a guillotine break. The bubble diameters vary between 50 and 140 mm
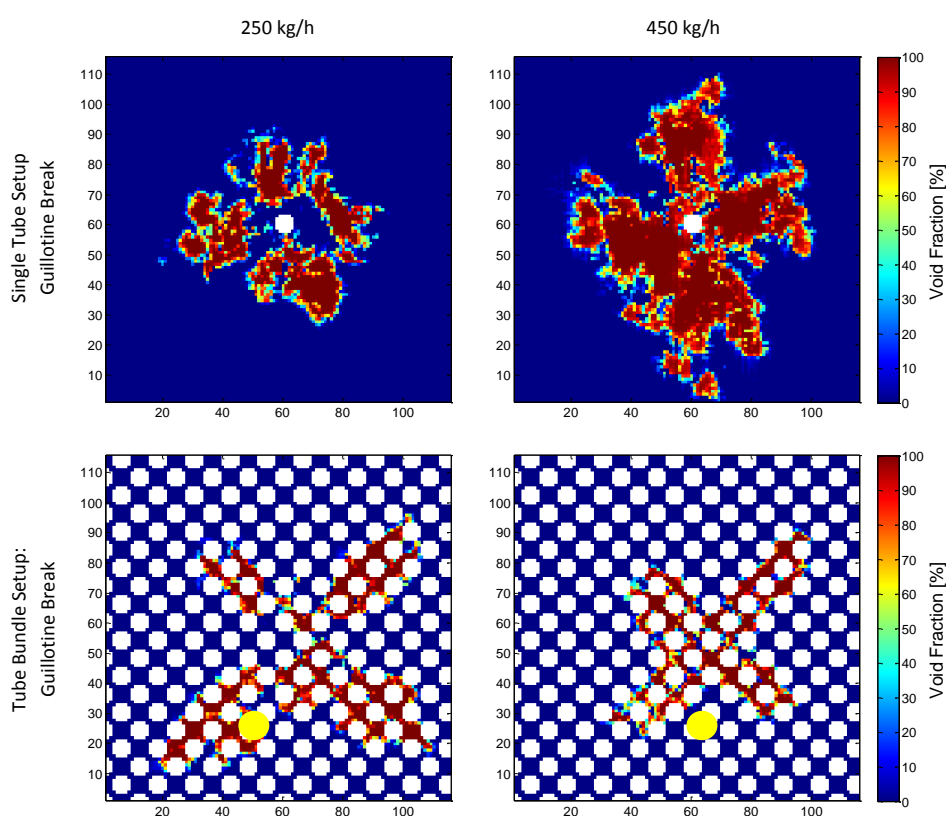
Figure 6: Sample void fraction frames for 100 mm measurement distance and two gas flow rates, 250 and 450 kg/h, with the single tube set-up, and with the tube bundle using the guillotine break. Injection tube is shown in yellow

3.1.4 Medium/long term stability of iodine in water pools

IRSN carried out experimental investigations of medium and long term stability of trapped iodine compounds in a pool scrubbing system. For this study the EPICUR facility, containing a ^{60}Co irradiator and allowing working with labelled iodine (^{131}I), was used. Online instrumentation by gamma counting is especially suited for this type of studies. A series of four tests in the EPICUR facility were performed to evaluate the medium and long term behaviour of iodine in water pools under irradiation. Laboratory tests were performed to improve the understanding of chemistry in solution (pH modification and component concentration) and the nature of the buffer under irradiation.

The laboratory test results showed that in unbuffered solutions, the pH drop is fast, combining the effects of radiolysis, oxidation and acid decomposition of thiosulfate. In buffered solutions (carbonate or borate buffer), radiolysis phenomena are initiators of the thiosulfate decomposition. Nevertheless, aqueous solutions preserve the buffering capacity for the tested irradiation durations (until 94h and ~272 kGy), which prevents

the formation of gaseous molecular iodine (I_2), but does not prevent thiosulfate decomposition in the very long term.

Four pool-scrubbing tests (PS) were carried out with unbuffered (PS1 and PS2 tests) and buffered (PS3 and PS4 tests) aqueous solutions to check the iodine volatility. Another parameter of interest for radiation stability experiments is the nature of the gas passing through the solution. Experiments were performed with air cover gas (PS1, PS2 and PS4 tests – PWR case) or with nitrogen cover gas (PS3 test – BWR case). The labelled aqueous solution was placed in the irradiation vessel. Before the irradiation phase, the vessel was heated to the set temperature (117°C) and pressure (~2.6 bar abs). Before irradiation, the vessel was maintained at the set temperature during 2 or 5 hours. During this pre-irradiation phase, the gas flowing through the irradiation vessel was air (the gas flow rate was 90 Nl/h). During the irradiation phase, the gas flowing through the irradiation vessel was either N_2 or air at 90 Nl/h. The temperature of the vessel was maintained at 117°C and the pressure at 2.6 bar abs. After the irradiation phase, the heating was stopped but the vessel was swept with dry air. The test matrix is given in Table 2 together with the final pH and the global iodine release values.

Table 2: PS tests - parameters and main results

Tests	PS1	PS2	PS3	PS4
Composition and Concentration (mol/l)	$Na_2S_2O_3$:$1.1x10^{-2}$ HCl : $3x10^{-5}$ HNO_3: $3x10^{-5}$ NaOH: $8.4x10^{-5}$ **I : $8.9 x10^{-11}$**	$Na_2S_2O_3$:$1.1x10^{-2}$ NaOH :$3.9 x10^{-4}$ HNO_3: $8x10^{-6}$ **I : $1.0 x10^{-7}$**	$Na_2S_2O_3$:$1.1x10^{-2}$ H_3BO_3 :$1x10^{-1}$ KCl : $5x10^{-2}$ NaOH $1x10^{-1}$ **I : $1.0 x10^{-7}$**	$Na_2S_2O_3$:$1.1x10^{-2}$ H_3BO_3 :$1x10^{-1}$ KCl : $5x10^{-2}$ NaOH $1x10^{-1}$ **I : $1.0 x10^{-7}$**
Initial pH	8.3	10.5	10.6	10.5
Activity (Bq)	$1.4 x10^8$	$1.1 x10^6$	$1.8 x10^6$	$9.6 x10^5$
Solution type	Unbuffered Solution Low Iodine concentration and medium pH	Unbuffered solution Alkaline pH	Buffered Solution (borate) Alkaline pH	Buffered solution (borate) Alkaline pH
Bubbling gas	Air	Air	N_2	Air
Irradiation duration (h)	11.5	21.7	27	40
Final pH	6.5	2.2	10.4	9.6
Global release* (%)	27 ± 3	97 ± 2	32 ± 3	51 ± 3

* The global release of iodine species corresponds to the difference between the activity of the solution after and before irradiation, it is expressed in percentage of the activity loaded in the solution before irradiation.

When the water pool is unbuffered, the iodine is released from the aqueous solution, essentially in inorganic form (I_2) expected to be the main inorganic species (but HOI could be present as well) and with a small proportion of species trapped in the quartz fiber filter (Figure 7). This release is due to the pH decrease; oxidation and radiolysis of thiosulfate induce a pH evolution to acidic values. The release is almost total and occurs very fast when pH is lower than 6.5. When the water pool is buffered (pH maintained over 9.5), no significant iodine release was observed on the dedicated filtering system (on-line Maypack). Nevertheless, according to PS4 test data, 51% of iodine mass was missing at the end of the test, combined with a significant evaporation of water and condensation on the Maypack. This would suggest a physical entrainment of water droplets towards the Maypack that would explain the loss of steam and iodine as they would have been transferred to the ventilation filter of the building. The interpretation of PS3 and PS4 tests with ASTEC V2.1 calculation code has shown that evaporating conditions with alkaline buffered solutions (even over pH=9.5) would lead to a significant gaseous HOI release whereas no I_2 would be released. The possibility to get gaseous HOI in significant amount has also been confirmed in the modelling of ACE-RTF [18] and PHEBUS-RTF [19, 20] tests at alkaline pH. Even if the experimental detection of gaseous HOI has still to be confirmed and pursued, these last results should be taken into account.
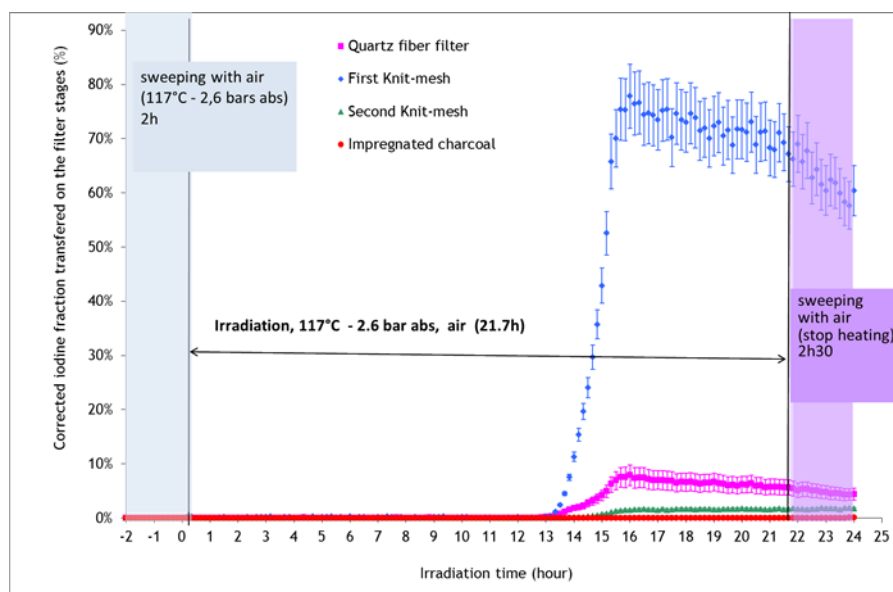
Figure 7: Evolution of the corrected total iodine fraction trapped on each filter stage (%) – PS2 test.

3.1.5 Retention of organic iodine in water pools

In the domain of FCVS wet filtration stages are often applied by different vendors. It is known from many experiments, that these pool scrubber systems feature a retention potential for different iodine species.

Previous state-of-the-art containment venting scrubbing solutions use a combination of sodium hydroxide or sodium carbonate with sodium thiosulfate in order to wash out volatile iodine species. Under severe accident conditions such volatile iodine species are aerosol bound iodide as well as gaseous compounds of elemental iodine, hydrogen iodide and organic iodide species (mainly CH_3I). With an alkaline thiosulfate solution high retention efficiencies for aerosol bound iodide as well as elemental iodine and hydrogen iodide are achieved. Nevertheless, the retention of gaseous organic iodide species in this solution is not satisfying and the search for improved organic iodine retention is ongoing.

One possibility for increased organic iodide retention potential of an FCVS is the enhancement of the retention in the scrubbing pool. The potential of scrubbers in general and the AREVA scrubber in particular in terms of organic iodide retention was investigated in this study by performance of parametric tests in a generic laboratory size test facility. The influence of the following parameters was experimentally investigated:

- Temperature of the scrubbing liquid solution (80 – 130 °C),
- Sodium thiosulfate (THS) concentration (0.2 – 3.5 wt%),
- Additives with the potential to enhance the phase transfer of hydrophobic compounds (e.g. CH_3I)
    - commercially available additive Aliquat 336® for 0.1 and 1 wt%,
    - Tween-80/Paraffin,
- Addition of mixing elements to the scrubber pool (Interpack®).

The tests were performed in the VESPER34 laboratory test facility of AREVA GmbH located in Erlangen, Germany. The test facility is situated in a controlled area and suitable for tests with tracered iodine.

Size and design of the VESPER34 test facility present a generic scrubber. The advantage of this small scale test facility is that operation conditions as well as scrubber liquid composition can be quickly modified at moderate costs. However, only qualitative results can be achieved which can only be compared with each other but which are not transferrable to the FCVS due to the small scale of the test facility. Mainly the limited flow rates at the inlet nozzle, the different shape of the small scale nozzle compared to the FCVS Venturi nozzle and the lower filling height (and lower surface area) lead to different (generally lower) retention efficiencies than in the FCVS.

The main results regarding CH_3I absorption efficiency of the test program are:

- No influence on the retention efficiency by a variation of the THS concentration;
- The absorption efficiency of the standard scrubbing liquid composition (0.5 wt% NaOH, 0.2 wt% THS) could be enhanced at higher temperature (130 °C) compared to 85 °C and addition of mixing elements (Interpack®);
- An enhanced retention was found by the addition of Aliquat 336® at temperatures below 110°C. This is in general accordance to the literature, but in VESPER34 tests the retention could only be enhanced up to a factor of 3;
- However the absorption efficiency of scrubbing liquid containing Aliquat 336® could not be further enhanced by addition of mixing elements at higher temperature. In fact at 130 °C the retention with Aliquat 336® even decreases;
- No influence of paraffin emulsion.

In general AREVA concluded that it was not possible to sufficiently improve the CH_3I absorption efficiencies by additional chemical compounds or by mixing elements. Consequently in case enhanced organic iodine retention is requested throughout the whole venting cycle, alternative and / or additional filtration methods such as dry filtration with a sorbent stage are necessary. This additional stage would also ensure high organic iodine retention rates and minimize significantly the organic iodine release to the environment.

3.2 Experimental Studies of Sand Bed Filters plus Metallic Pre-filters

IRSN carried out experimental investigations of medium and long terms stability of several iodine compounds trapped in different filtration media currently implemented on the French Nuclear Power Plants, *i.e.*, sand bed filters and metallic pre-filters. For this study, various IRSN facilities were used: i/. the EPICUR loop (Cadarache), containing a ^{60}Co irradiator and allowing working with labelled iodine (^{131}I), knowing that online instrumentation by gamma counting is especially suited for this type of studies; ii/. the BRIOCH test bench (Saclay), a laboratory scale set-up dedicated to study filtration efficiency of methyl iodide (^{127}I) species; iii/ the IRMA facility (Saclay), containing ^{60}Co sources for irradiation of various components.

A series of three tests in the EPICUR facility was performed to evaluate the medium and long terms behaviour of caesium iodide aerosols previously deposited respectively in the sand bed filter (2 tests) and the metallic prefilter (1 test). Preliminary laboratory tests involving iodine aerosols and molecular iodine were performed to qualify the generation process and the experimental protocol of iodine "loading" phase into the filtration media.

Some main conclusions can be drawn concerning the sand bed filter:
- A sand filter alone, dry or wet, is not able to trap significantly molecular iodine. Some additives may improve the situation but this needs to be deeper investigated. Anyway, release of trapped molecular iodine under irradiation could not be tested.
- A sand filter traps CsI aerosols with high efficiency, even if the objective here was not to quantify the precise decontamination factor. Release of the trapped CsI under irradiation was tested twice, one test with dry sweeping gas (SF1) and another one with wet air (SF2). In both cases, for a temperature between 100 and 120°C a significant "thermal release" begins before the irradiation onset (and under dry conditions), confirming a thermal contribution of the CsI decomposition process. As indicated in Figure 8, the thermal inorganic release is significantly more important for SF2 than for SF1 and remains to be explained.

This release goes on under irradiation at rates close to 1% per hour for both tests. The final released iodine fraction reaches 42% for the experiment performed in completely dry conditions (SF1 test, see Figure 8) and 61% for the experiment performed with humidity (SF2 test, see Figure 8). In both cases (SF1 & SF2 tests), inorganic iodine is the main released chemical form. A modelling of CsI deposit through a radiolytic process shows that CsI radiolytic decomposition rate is consistent with these tests and also with other tests performed in the frame of OECD-STEM project [21].

Concerning the metallic pre-filter experiments, the different preliminary tests confirmed that molecular iodine is significantly retained on a representative section of the original filtration cartridge (purchased from PALL® and made of stee with a geometric surface of 244 cm² whereas the real surface seen by iodine is estimated to be close to 7500 cm²) and that the gas flow rate through the metallic pre-filter is a key parameter

for retention. Specific attention was paid on the stability of CsI aerosols trapped on this kind of filter. The main insights are that the metallic pre-filter traps efficiently CsI aerosols and that the global release under irradiation (tested with wet air) does not exceed 0.2% of the initial value. This very low release is entirely found under gaseous molecular iodine form. Compared to sand filter experiments performed in similar conditions, inorganic iodine should be formed in significant amounts as CsI decomposes under irradiation. As the final iodine release from a metallic prefilter is hundred times less, it is likely that inorganic iodine was formed in significant amount by CsI thermal-radiolytic decomposition and then efficiently trapped in the metallic pre-filter due to its high specific surface area.
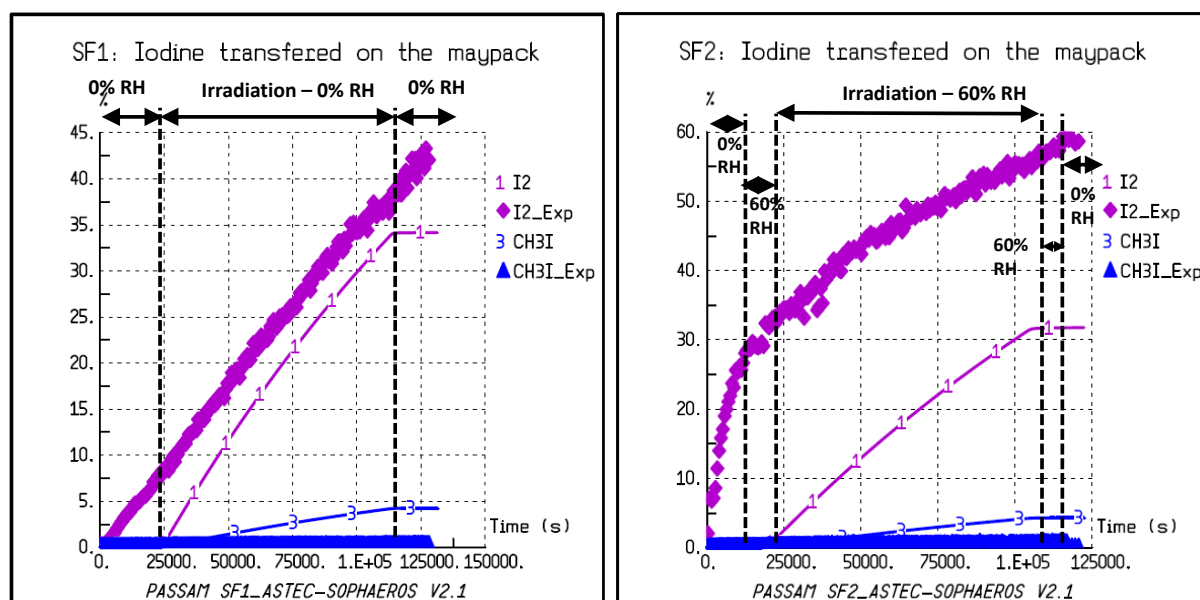

Figure 8: Evolution of the corrected iodine fraction trapped on each filter stage (%) for SF1 and SF2 tests and the corresponding modelling performed with ASTEC-SOPHAEROS V2.1 calculation code.

Complementary studies would be needed to get more quantitative assessments, and to test species other than CsI. An important point is that the release of gaseous iodine from CsI aerosols trapped in a sand bed filter, as observed in these tests, may cause a delayed iodine source term after the operation of such a FCVS.

Methyl iodide trapping efficiency was also investigated on sand samples using the BRIOCH test bench including a PDECD (Pulsed Discharge Electron Capture Detector) gas chromatograph. The sand samples were prepared with various additives in order to try enhancing the retention capabilities for methyl iodide. Some of these samples were irradiated in the IRMA facility. In none of the tests, taking into account the uncertainties of the experimental setup, any retention of methyl iodide could be measured. The same conclusion arose when coarse stainless-steel wool was challenged by $CH_3{}^{127}I$ in air as a carrier gas.

3.3 Experimental Studies of Acoustic Agglomeration Systems

Aerosol Acoustic Agglomeration (AAA) [22] is one of the innovative techniques not considered in current designs of FCVS and investigated within the PASSAM project.

The AAA is a process based on the interaction of the sound waves and the suspended particles in an aerosol. Under specific conditions a variety of physical mechanisms can bring some of the particles together and produce collisions that may lead to a coagulation process known as acoustic agglomeration. The main mechanisms involved are the orthokinetic effect [23], the scattering [24], and the so-called mutual radiation pressure [24].

Due to the lack of information about the experimental behavior of acoustic agglomerators in scenarios as those postulated within a severe accident, CSIC (Spain) and CIEMAT (Spain) have collaborated to integrate a Mitigative System Acoustic Agglomerator (MSAA), designed and developed by CSIC, within the PECA (Platform for Experimental Characterization of Aerosols) vessel in the Laboratory of Analysis of Safety

Systems (LASS) at CIEMAT. This setup has been designed to study the application of AAA under conditions anticipated during filtered containment venting [25].

The AAA experimental campaign was conducted at the PECA-MSAA facility (Figure 9). The aerosol characteristics were adapted to those of the expected aerosols in the nuclear event as much as allowed by the generation system. The details of the system are described elsewhere [26]. The MSAA generated a 21 kHz standing wave field inside the chamber with an average sound pressure level of 155 dB. The ultrasonic generators were of the kind of airborne power stepped-plate transducers with electronic resonance control. The gas flow that carried the aerosol through the acoustic chamber was air with a flow rate between 12.5 kg/h and 200 kg/h. The aerosols were constituted of TiO_2 and SiO_2 particles of 0.3, 1, and 2.5 µm. Twenty experiments were carried out with the features summarized in Table 3.
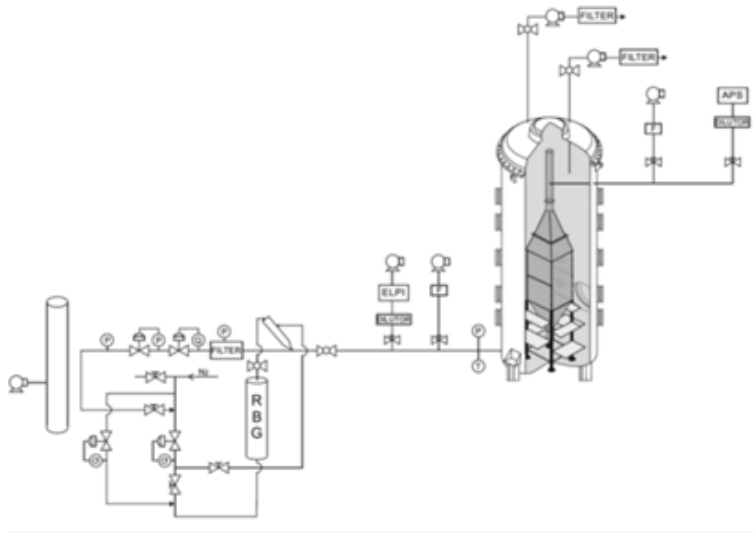

Figure 9: Lay-out of the PECA-MSAA facility

The procedure followed in the experiments was divided into several steps. First there was a stabilization step in which the aerosol generation was monitored at the inlet by an electrical low-pressure impactor (ELPI device). After reaching stabilization the second step consisted of the measurement of the aerosol particles at the outlet of the MSAA by means of an Aerodynamic Particle Sizer (APS). Such measurements were carried out with and without ultrasounds. Each experiment was repeated once.

To compare the particle number concentration at the inlet and at the outlet the two different counters (ELPI and APS) were used only in the common size range. The effect of ultrasound on the particle number was quantified by using the following equation where Np_b is the relative particle number during the phases with and without ultrasound and RC_{Np} is the number reduction coefficient.

$$RC_{Np} = \left(1 - \frac{mean\,(Np_{b\ with\ US})}{mean\,(Np_{b\ without\ US})} \right) * 100\%$$

Experimental results confirm that ultrasound agglomeration effect improves with particle number concentration and size dispersion and is proportional to acoustic intensity and treatment time. For treatment times of about 80 seconds and particle number concentrations in the range $10^4 - 10^5$ cm^{-3} the smaller particles (0.3 microns) experiment a reduction of over 90% with an acoustic intensity of about 155 dB. Under the same conditions the increase of the particle size due to ultrasound was mainly observed for 1 µm particles in which increases of up to 37% were measured.

In addition, a numerical model, based on the fundamental interaction effects acoustic waves – aerosol particles, was developed in MATLAB code and experimentally validated. From the model the acoustic power required in case of a severe accident could be established for a particle number reduction of 90%.

Table 3: Experimental matrix for Aerosol Acoustic Agglomeration tests

Name	Flow rate [kg/h]	Treatment time [s]	Mass Concentration Input [mg/m³]	Input Mass Proportion (%)			
				SiO₂ 0.3 μm particles	SiO₂ 1 μm particles	SiO₂ 2.5 μm particles	TiO₂ particles
AAA2	100	10	25	0	100	0	0
AAA6	100	10	25	75	25	0	0
AAA5	50	20	50	75	25	0	0
AAA4	12.5	80	200	75	25	0	0
AAA1	12.5	80	200	0	100	0	0
AAA3	12.5	80	200	50	50	0	0
AAA7	12.5	80	200	90	10	0	0
AAA8	12.5	80	200	0	75	25	0
AAA9	12.5	80	200	50	30	20	0
AAA10	12.5	80	200	50	30	0	20

Note: header uses SiO_2 and TiO_2.

3.4 Experimental Studies of High Pressure Spray Agglomeration Systems

High pressure sprays have been used in multiple industrial applications, including NPPs (High Pressure Core Spray System of BWR/5 and BWR/6). In nuclear reactors, low pressure water sprays are widely installed as engineering safety systems to depressurize the containment but these systems are also considered capable of capturing particles from the containment atmosphere. The study, developed in RSE, is dedicated to verify the efficiency on particle capture of an innovative device based on a high pressure spray system and to develop and evaluate a simplified spray model for aerosol removal rate. This system works with pressure from 50 to 130 bar. Two different measurement campaigns were done: the first one was about a characterization of the spray droplets with a non-invasive optical method and the second one was devoted to evaluate the aerosol removal rate of the high pressure water spray systems. The tests were performed using a single nozzle in order to simplify the investigated phenomena.

The size distribution and velocity of the droplets are measured using a non-invasive measurement technique called Phase Doppler Anemometry (PDA) that uses the properties of coherence and polarization of two crossing laser beams to measure the velocity and the size of the water droplet passing through it. These data are used as initial condition for the model of droplet size and velocity evolution and to validate its output. Measurements are carried out with the spray axis oriented vertically downwards, along 5 cross patterns traversing diametrically the spray, located perpendicular to the spray axis at the axial distance of 50, 100, 250, 500 and 750 mm respectively from the injection nozzle. The water pressures are 50, 80, 100 and 130 bar and the flow ranges between 0.8 and 1.3 l/min.

The droplet size distribution in the injection zone has a peak between 25 and 35 μm and the droplet velocities are between 100 m/s and 50 m/s according to the different pressures. The droplet size increases during the fall of the droplet due to an agglomeration phenomenon as reported in Figure 10(a) and there is a progressive loss of their velocity due to momentum exchange between droplets and air (Figure 10(b)). The velocity decreases down to 10 m/s at 750 mm from the nozzle for different pressure.
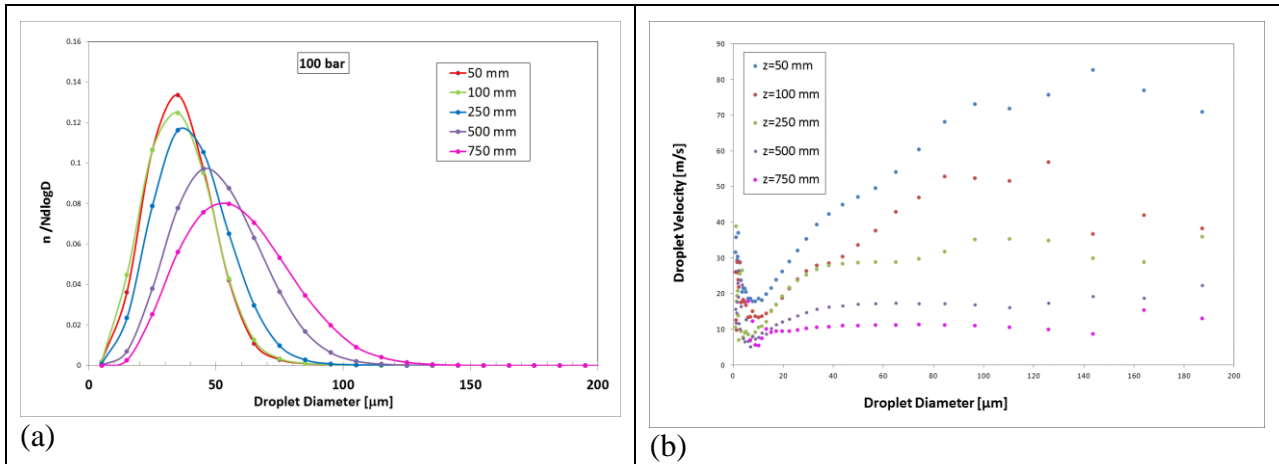
Figure 10: droplet size distribution (a) and droplet velocity distribution (b), at 100 bar at different distances from the nozzle

The second test campaign was carried out in a purposely built facility (SCRUPOS) composed of a scrubbing chamber of 0.5 m x 1.0 m and 1.5 m high, with glass walls to permit the complete view of the aerosol removal process. The aerosol was injected to form a cloud of specific particle concentration. The chamber was equipped with a high pressure water spray system with a single nozzle placed on its top and a sample line for concentration measurements (Figure 11(a)). The spray was kept running for 2 min and the efficiency of the aerosol removal was evaluated, along the test time, using an optical particle sizer (OPS) that acquires particle concentration over 16 channels from 0.3 to 10 μm. The tests were performed with powders composed of SiO_2 particles with mean size of 0.4 μm, 1 μm and 2 μm, with different water injection pressures (50, 100 and 130 bar) and different initial particle concentrations (ranges: 2-90 mg/m^3).Tests showed that the removal rate λ (defined by $\frac{C(t)}{C(0)} = e^{-\lambda t}$ with C(t) = concentration at t time and C(0) = initial concentration) is not influenced by the initial particle concentration, it depends on aerosol size and it linearly increases with increasing water injection pressure (Figure 11(b)). This occurs because an increase in the water pressure provides a higher flow rate and smaller droplets leading to an increased efficiency for impacting aerosol particles and a higher density of droplets. The removal rate and the half life time (the time necessary for the concentration to halve) at 130 bar for different aerosol sizes are reported in Table 4.

Table 4: Removal rate and half-life time for different aerosol sizes at 130 bar pressure

Aerosol size [μm]	$\bar{\lambda}$ [1/s]	Half-Life time [s]
0.4	0.064± 5%	11
1	0.116 ± 5%	6
2	0.19 ± 17%	3.6

A simplified model provides the droplet size distributions, the droplet velocities, the air velocity and the particles concentration based on droplet–droplet and droplet-aerosol interaction. The developed model shows a good agreement with the experimental data. The removal rate depends on the efficiency of particle capture by water droplets. The capturemechanisms are inertial impaction, interception, Brownian diffusion, thermophoresis and diffusiophoresis. In our experiments, since gas and water are at room temperature, the thermophoresis and diffusiophoresis effects are not considered. The inertial impaction effect is dominant for big particles up to a few microns, then the main phenomenon is the interception and for aerosol particles smaller than 0.3 μm the Brownian diffusion is the primary effect. Considering the experimental condition (at 100 bar – mean droplets size 40 μm and velocity 30 m/s), the removal rate is calculated using different models developed by Powers (potential regime (droplet Reynolds number→ ∞), viscous regime (droplet Reynolds number→ 0), and transitional regime) [27] and by Porcheron [15] with and without inertial impaction. The experimental data are better described if the inertial impaction contribution is not considered (Figure 12). The fitting is good but it was noticed that the results are sensitive to droplet diameter.
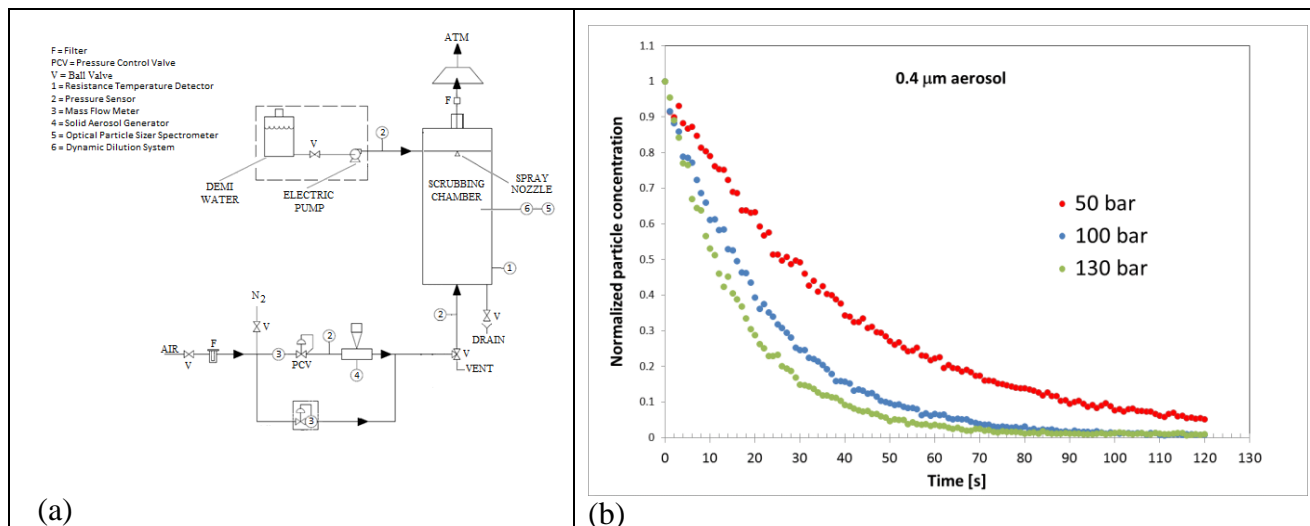
Figure 11: (a) SCRUPOS layout, (b) trend of 0.4 μm aerosol normalized concentration during water spray at different spray pressures.
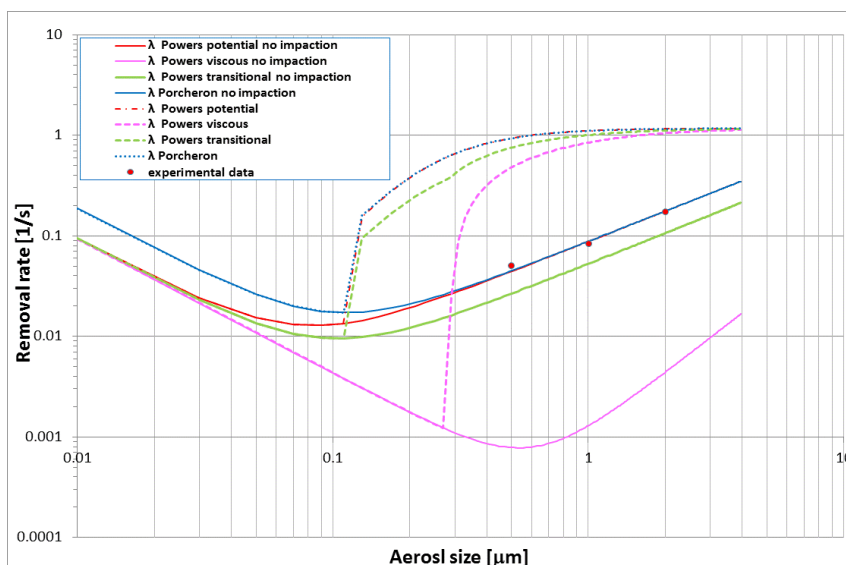
Figure 12: Removal rate according to different capture models: model developed by Powers [27] for potential regime (red dot line), viscous regime (pink dot line), and transitional regime (green dot line), and model reported by Porcheron, that have a different Brownian contribution, [15] (blue dot line), all of them considering the three effects (inertial impaction, interception and Brownian diffusion- dashed lines) and without inertial impaction (full lines) and experimental removal rate at 100 bar (red dots).

However, few studies have addressed this potential capability and most of the researches on spray performance have been conducted for low pressure sprays. Therefore, high pressure spray application either as an additional system to decrease aerosol concentration or as an agglomerator in the pre-filter stage of a FCVS requires new specific studies.

With regards the comparison between low and high pressure spray on aerosol removal, the half-life of 1 μm particles within the high-pressure spray chamber, turned out to be 50-100 times shorter than the half-life observed in a low-pressure spray system applied for removing a similar aerosol cloud. Within the sample volume of the chamber, it was found that a single-hole spray nozzle operating at 130 bar, can remove at least 99.9 % of suspended micron sized particles in a time of the order of a minute (about 1 minute for 1 μm particles, about 2 minutes for 0.5 μm particles). No influence of the initial aerosol concentration was observed for both 1 μm and 0.5 μm particles. When compared to low-pressure sprays, the removal efficiency

was much higher, which encourages the application of this high-pressure technique in multi-nozzles and multi-stages configurations.

3.5 Experimental Studies of Electrostatic Precipitators

Potential of electric filtration systems was discovered early in the 20th century, when corona discharge was found to remove particles from gas streams. Today many types of these filters exist including electrostatic precipitators (ESP), air ionizers and ion wind devices. Typically they are very efficient filtration systems with minimal resistance to the gas flow. They are applied for reduction of many industrial emissions, including those from coal and oil fired power plants, salt cake collection from black liquor boilers in pulp mills, and catalyst collection from fluidized bed catalytic cracker units in oil refineries.

An ESP removes aerosols from gas flow due to forces induced by strong electric fields [28]. In case particles do not get high enough charge for their collection, a pre-charging water mist can be sprayed to enhance particle growth in diameter and charging. This system is called Wet ESP (WESP). The operation temperature of a typical WESP at atmospheric pressure is limited to 90 °C and the pressure drop through the system is small. The reported energy requirement for gas filtration by ESP varies from 0.01 to 1 $W.h/m^3$. The atomization of water is probably the main power drain of WESP. In case of the atomization of small droplets, it is approximately $0.1 - 0.2$ $W.h/m^3$.

Typical collection efficiency of a WESP for particles is between 99 to 99.9 %. Nonetheless, collection efficiency can be increased by maximizing the strength of the electric field [29] and the residence time within the precipitator. Other factors affecting efficiency are dust resistivity, gas temperature, chemical composition (of the dust and of the gas flow), and particle size distribution. WESP performance has been hardly tested for gaseous iodine, although preliminary tests on gaseous iodine filtration were conducted by VTT in 2011. In this case higher efficiency might be reached by adding an oxidation stage (ozone generator) that turns gaseous iodine species into iodine oxide particles.

Application of WESP under the foreseen conditions of a nuclear severe accident poses major challenges, notably the filtration of iodine volatile species including organic iodides.

In order to filter gaseous iodine, an innovative technique involving four steps has been developed by VTT, and further tested in this project. The first step is the oxidation of gaseous iodine into iodine oxide particles by ozone [30, 31, 32]. The second step is the growth/agglomeration of the formed iodine oxide particles and the coagulation of particles with sodium hydroxide droplets (NaOH dissolved in water). Particulate iodine is dissolved in the droplets, whereas gaseous iodine is absorbed by the droplets. As iodine oxides particles have coagulated with droplets or agglomerated with other particles, the iodine oxide particles grow in diameter and thus the filtration efficiency is also increased. The third step concerns the behavior of iodine in an electric field of ESP. Corona discharges from the needle-like electrodes are relatively low power electrical discharges that take place at or near atmospheric pressure. The corona is invariably generated by strong electric fields associated with sharp needles. The ions from the corona serve to charge individual particles and droplets as the gas flow carries them through the ESP. Then, these charged particles and droplets drift to the collection electrode due to the electric field. The last step is the flushing of ESP wall surfaces. At the ESP stage, the collection electrode surfaces of the precipitator are kept clean by flushing with sodium hydroxide solution (doped with sodium thiosulfate $Na_2S_2O_3$ for the experiments with methyl iodide).

Several series of tests have been performed by VTT and the following points can be stated. From tests at room temperature conditions, using TiO_2 aerosols, a strong decrease of the trapping efficiency for voltages below 15 kV (negative) was evidenced (Figure 13).

Using gaseous and particulate iodine, the optimum parameters related to the operation of the applied WESP have been determined (number of corona needles, effect of the flow-rate, etc...) leading to a very good efficiency for gaseous I_2 filtration in "dry" atmosphere (i.e. without steam content) (Figure 14).
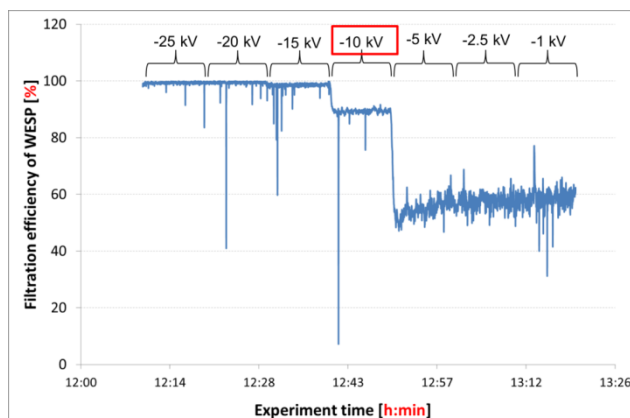
Figure 13: Filtration efficiency of TiO₂ particles for a volumetric flow rate of 86 l/min in the WESP and several applied voltages.
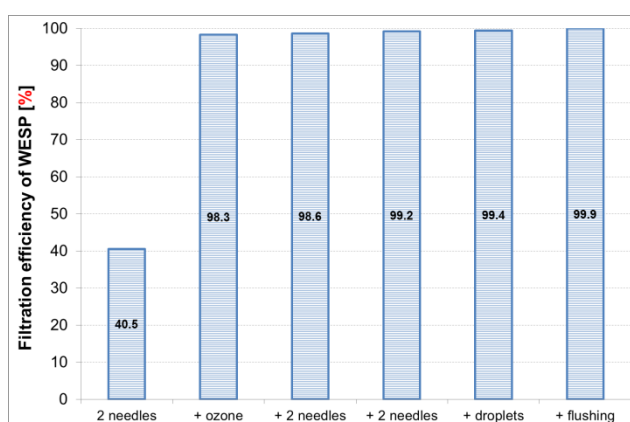

Figure 14: Filtration efficiency of the WESP, calculated on the basis of particle number concentration measurements with ELPI

Other tests have been performed at higher temperature (60 °C) in presence of steam, confirming the utility of different process steps (oxidation of I_2 or CH_3I into iodine oxide (IO_x) particles, spraying of NaOH droplets, flushing of electrical filter wall) [33].

The filtration efficiency for gaseous molecular iodine (I_2) based on the particle number was higher than 99.5 %. Since the high efficiency was observed for three flow rates of steam, it was difficult to point out the effect of increasing steam content in the carrier gas. The high filtration efficiency was observed for the whole range of particle diameters recorded in the ELPI measurements (Figure 15). The efficiency of the first step (oxidation of gaseous iodine) was confirmed because at the inlet of the facility, 96 % of iodine mass was in the form of particles and 4 % was in the gaseous form, thus most of the molecular iodine had been transformed into I_xO_y particles.

The filtration efficiency of a higher concentration of gaseous molecular iodine based on the particle number was higher than 95 %. The filtration efficiency was decreased for the particles with a diameter of 0.1 – 0.2 μm. Increasing the amount of steam in the carrier gas increases the retention of iodine in the WESP. However, increasing the initial amount of I_2 tends to decrease the filtration efficiency.

The filtration efficiency for methyl iodide based on the particle number was higher than 82.6 %, which is lower than in the case of molecular iodine. Increasing the steam fraction in the carrier gas tended to decrease the filtration efficiency for the particles. The results from ICP-MS measurements showed very low filtration efficiency (> 41 %) for the total mass of iodine (gas and particles). At the inlet of the facility, only 5 % of iodine was in the form of particles and 95 % was in the gaseous form. The most probable explanation in these different behaviors between methyl iodide and molecular iodine can be found in the size of the particles. The particles formed from methyl iodide may be smaller, due to the lower vapor pressure, and consequently the particles decompose more easily or the particles need shorter time for the decomposition.
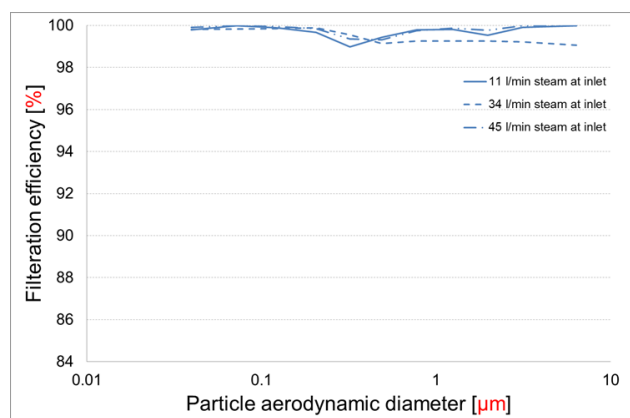
Figure 15: Filtration efficiency of the WESP (at -25 kV) as a function of particle aerodynamic diameter, calculated on the basis of particle number concentration measurements with ELPI

Despite this last result showing a non-satisfactory efficiency for organic iodine, the work has shown that VTT´s innovation to use "ozone feed and WESP" together enables the filtration of both gaseous molecular iodine and iodine containing particles (e.g. I_xO_y). However, it has to be kept in mind that the filtration efficiency strongly depends on the WESP design/geometry optimization. The location of the oxidation step closer to the WESP inlet needs to be further tested in order to avoid possible particle decomposition before the filtration step and consequently, to increase the filtration efficiency against organic iodine.

3.6 Experimental Studies of Improved Zeolites

In order to mitigate atmospheric releases in case of a severe accident on a NPP, an efficient solution may consist in combining current filtration devices (wet scrubbers, sand bed filters…) with an additional filtration stage made of inorganic porous adsorbent. In that respect, zeolites are obvious candidates thanks to their thermal stability and radiation resistance, high specific surface areas, tunable pore size and chemistry.

The generic objectives of the study were: (i) to establish structure-activity relationships between the chemical, textural and structural properties of silver zeolites and retention performances towards I_2 and CH_3I; (ii) to study the most interesting zeolitic formulations under conditions close to those met in a severe accident; (iii) to examine the trapping mechanism.

Extensive syntheses (up to 18 made by ion-exchange or impregnation from 5 different structures, namely silver-zeolites), characterizations and testing of zeolitic sorbents were achieved at University of Lorraine. Overall, the effect of various zeolitic parameters (pore structure, chemical properties, silver content and speciation) was determined by combining quantitative data collected during iodine gas-phase dynamic retention tests (adsorption capacities, decontamination factors, trapping stability) together with physico-chemical characteristics obtained from characterization studies (elemental analyses, N_2 sorptiometry at 77K, XRD, DRIFTS of adsorbed CO, DR-UV-Vis spectroscopy, electron microscopy…). Zeolitic formulations, which have shown the best retention behavior under simplified conditions (high concentrations of I_2 or CH_3I, absence of inhibitors, T=100°C), were then selected for additional tests in order to extrapolate to severe accident (SA) conditions (low iodine concentrations, irradiation, different temperatures, presence of humidity, COx, NOx, H_2, Cl…), through a collaborative work between University of Lorraine and IRSN (Saclay and Cadarache). The trapping mechanism was also investigated through using *in situ* spectroscopic techniques and after-test characterizations.

1) Parametric study

Preliminary experiments on the effect of the exchanged cation have shown that silver zeolites were the most efficient towards the capture of CH_3I. By contrast, other cationic forms (Pb^{2+}, H^+) displayed rather poor retention performance while copper-exchanged zeolites were found to be rather unstable and to promote the release of I_2 by redox processes. Hence, a peculiar attention was devoted to silver zeolites in order to gain insights onto the following aspects: (i) the effect of the pore size/connectivity according to the structural type; (ii) the silver content; (iii) the silver speciation and preparation method (exchange or impregnation).

By considering adsorption capacity only, the most prominent factor towards CH_3I retention is the amount of silver that could be deposited in dispersed form (as Ag^+ cations or small embedded clusters, by contrast with silver nanoparticles obtained by impregnation at high Si/Al ratio, Figure 16(A)). Such a high silver content may be achieved through repeated ionic exchanges with zeolitic materials, such as faujasite, having high cationic exchange capacity (Si/Al <5).

A specific testing procedure was elaborated with the aim of distinguishing the fractions of volatile iodine trapped reversibly (blue bars on Figure 16(B)) or irreversibly (chemisorbed CH_3I (green bars) and as AgI precipitates (red bars, Figure 16(B)). Among all the investigated zeolitic materials, a large pore faujasite zeolite (of Y type) with 23 wt% of silver "*22.8Ag/Y (2.5)*", displayed the best retention performances towards volatile iodine species (Q_{sat} = 209 mg/g and 380 mg/g for CH_3I and I_2 respectively at 100°C, DF = 10^5 during 9 days with $[CH_3I]_0$ = 1 ppm, up to 80% of storage under thermally stable and insoluble AgI precipitates). Therefore, a special attention was paid to this zeolite in order to assess the effects of temperature, irradiation, inhibitors and also to carry out an in-depth study of trapping mechanisms.
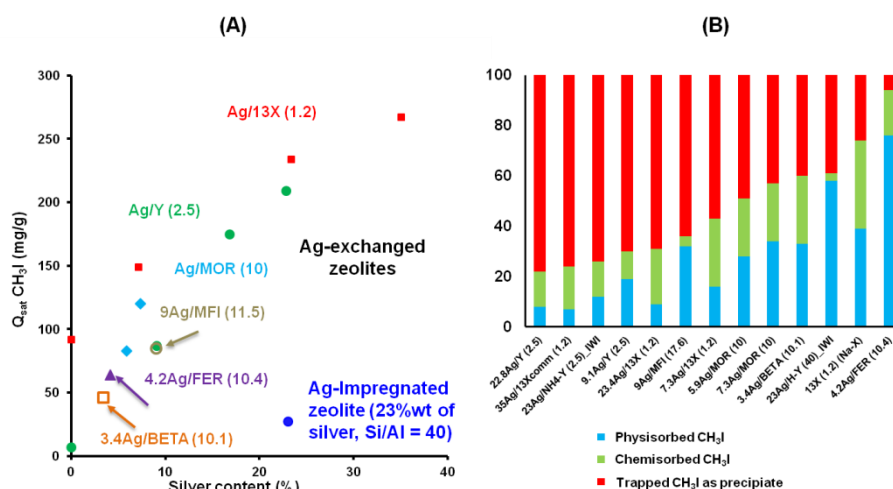

Figure 16: (A) Evolution of CH_3I adsorption capacity as a function of silver content (T=100°C, absence of contaminants) and (B) relative distribution of trapped CH_3I species for different silver-zeolites.

2) *Extrapolation to SA conditions*

The adsorption temperature was found to have only little influence on the CH_3I sorption properties of Ag/Y sorbent in the range of 35-250°C, the production of catalytic by-products (oxygenates, higher hydrocarbons) being promoted at the expense of physisorption at higher temperatures.

The impact of irradiation was studied at IRSN by two different procedures. First, an irradiation (total dose of 1.14 MGy; ^{60}Co source, IRMA facility) was performed before test. This pre-treatment did not change the physico-chemical characteristics of the sorbent and its retention performances towards I_2 and CH_3I. On the other hand, the trapping stability of I_2 under irradiation and in very humid conditions (T =120°C, dose rate of 2.9 kGy/h, R.H = 60%, 29 hours) has been also checked (EPICUR facility at IRSN-Cadarache) using a commercial silver faujasite (X type) with 35%wt of silver. No measurable release of iodine species was observed confirming therefore the high stability of trapping thanks to the formation of stable and insoluble AgI precipitates.

The effect of some potential inhibitors (CO_x, NO_x, H_2O, H_2, chlorinated species) present under SA conditions was also investigated. Nevertheless, it should be acknowledged that additional tests should be performed in more representative conditions (mixture of inhibitors, more representative concentrations, irradiation…) to be conclusive. Under the experimental conditions employed (T=100°C, CH_3I:CO = 5:1, CH_3I:H_2O = 1:8, CH_3I:H_2 = 1:12.5), the presence of CO, H_2O or H_2 in the feed gas had only little or no impact on CH_3I retention. However, the presence of NO_2 (CH_3I:NO_2 = 2:1) induced a significant oxidation of CH_3I to I_2. This problem can possibly be overcome using a second sorbent bed (Pb/zeolite for example). It may also be necessary to carry out further studies to evaluate the effect of chlorinated species since they

promote some poisoning of active silver sites (by formation of AgCl), making them less efficient for iodine trapping.

Finally, a "large scale" test for measuring a global DF on a commercial silver-exchanged zeolite was performed on the new IRSN PERSEE facility and confirmed the good retention efficiency for CH_3I.

3) Trapping mechanism of volatile iodine by silver zeolites

For the first time, a combined spectroscopic approach using gas-phase FTIR, *in situ* DRIFTS and *in situ* DR-UV-Vis spectroscopy was used to unravel the CH_3I trapping mechanism on silver zeolites. Detailed mechanistic schemes relevant to: (i) the nucleation and growth of AgI precipitates in the zeolite cages; (ii) the catalytic decomposition of CH_3I to different by-products, whose relative distribution seems to be affected by zeolitic structure, were obtained [34].

4) Conclusion

This study represents a significant improvement in the knowledge of silver zeolites in the context of severe accident. Overall, sorbents prepared by ionic exchange with silver in faujasite Y (especially with 15-23 wt% Ag) displayed the highest performances for the retention of CH_3I and I_2. A commercial Ag/X zeolite with 35wt% silver had also good properties, but partially-exchanged Ag/X zeolites (with lower Ag content and higher Na content) are less suitable and also more sensitive to humidity (too low Si/Al ratio). Silver zeolites with small pores, such as ferrierite (FER), promote reversible adsorption and are not recommended. By contrast, other kinds of zeolitic structures with medium to large pores (mordenite, MFI)) behave rather well. Overall, increase of the silver content in silver-exchanged zeolites improves both the adsorption properties and trapping stability. Nevertheless, a silver content about 9-10 wt% may be enough due to the high cost of silver. The behaviour of the studied faujasite silver zeolites under extrapolated severe accident conditions was found to be interesting, meeting the mitigation target, even if the effect of some potential inhibitors remains to be determined on a wider range of conditions.

3.7 Experimental Studies of "Combined" Filtration Systems

In AREVA's FCVS standard a Venturi scrubber section is combined with a metal fiber filter (MFF) stage. A combination of processes with complementing characteristics results in a robust design with constant high retention efficiencies for aerosols and inorganic volatile iodine over the integral venting operating range.

For an enhanced organic iodine retention in the FCVS AREVA has looked into different possibilities. Enhancement of the scrubber solution showed little potential to reach high organic iodine retention efficiencies (at least for decontamination factors DF > 10) in the performed laboratory screening tests. Consequently, in order to ensure high retention rates and minimize significantly the organic iodine release to the environment throughout the whole venting cycle, additional filtration methods such as dry filtration with a sorbent stage and passive superheating device were investigated.

As sorbent a zeolite structure impregnated with $AgNO_3$ was chosen. Next to high efficiency with cost optimized silver content its hydrophobic characteristic, high chemical, thermal, mechanical stability and radiation resistance are favorable for the FCVS process.

Large scale organic iodine retention tests were conducted at the JAVA PLUS test facility to measure the retention efficiency of the complete process section consisting of Venturi Nozzle (VN) section, MFF section, throttling orifice and additional sorbent stage.

During the large-scale tests the organic iodine retention performance (CH_3I) was measured covering the complete venting cycle. Next to system inlet pressure from 1.5 to 8 bar abs the temperature, superheating, steam content, flow velocity and pressure in the sorbent section were varied. In addition transients such as start-up of the venting system and boundary conditions were investigated.

The main parameters found influencing the retention efficiency are superheating (dew point distance) and residence time in the sorbent bed. Based on the found relationships, the dimensions of the sorbent stage can be adjusted by empirical correlations to meet the requirement of different authorities or customer request regarding the DF for organic iodine. Thereby the qualification ensures reliable and verified performance values by excluding relevant scaling errors from lab scale to industrial application. In addition the passive superheating by isenthalpic throttling was verified.

Based on the results at the JAVA PLUS test facility, there are 2 possibilities for the implementation of the FCVS PLUS (presented in Figure 17):

- Combined vessel with the 3 filtration stages included;
- Split version: separate vessels for the different stages (for example for retrofitting or space issues).
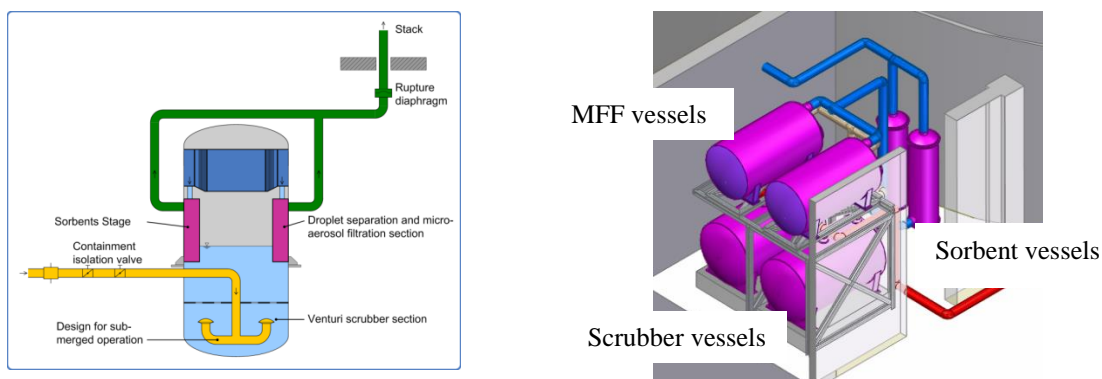

Figure 17: Schema of an AREVA FCVS PLUS with integrated sorbent section (left) and as split vessel design (right)

The final design of the FCVS PLUS is optimized regarding:

- Minimization of heat losses between the orifice and MSS;
- Minimization of pressure drop over the MSS;
- Optimized flow and temperature distribution in the sorbent (even residence time over the flow cross section);
- Optimized design of the molecular sieve section (inlet section, outlet section, flow distribution, arrangement in an integral vessel as well as separate vessel).

The performed lab scale tests covering harsh environmental conditions complete the qualification of used sorbent material for severe accident conditions. The sorbent material is qualified concerning stability at stand-by (cold and hot) and at operating conditions against pressure, humidity, gas composition, etc. as well as thermal and radiation resistance.

The corresponding results, summarized in this report are detailed in a specific PASSAM report [35].

In summary, under all operating conditions, the CH_3I-retention in JAVA PLUS tests was in the expected range of approximately 98 % (DF 50) or in most cases far above for the used sorbent section dimensions. The collected values were used for the elaboration of the methodology to design the molecular sieve section. In addition the adsorption filtration section also improves the retention of inorganic volatile iodine as such species are also bound with high efficiency on the used adsorbent.

3.8 Experimental data analysis and development of models and correlations

Finally, one of the last - but of primary importance - step in the PASSAM project consisted of an in-depth common analysis of the experimental results in order to better understand the studied phenomena and, when applicable, to draw simple models and correlations which, should be later implemented in severe accident codes such as ASTEC [3] or in more specialized codes, in particular those related to pool scrubbing. The objective was to improve these codes in the domains for which gaps of knowledge had been identified through the PASSAM state of the art report [4] and so to enhance their capabilities of modelling Severe Accident Management scenarios and developing improved guidelines.

Some major outputs from this analysis and interpretation work have been shortly mentioned in the previous sections together with the corresponding experimental results. They are detailed in [36] and not reproduced in this section of the present synthesis report. Nevertheless the following conclusive section of this synthesis report takes widely into account the outcomes of this interpretation work.

4 CONCLUSIONS

PASSAM experimental studies were performed for improving mitigation systems (FCVS) in case of severe accident on a nuclear power plant. The experimental studies were performed both for existing systems (i.e., water scrubbing (PSI, CIEMAT, RSE, AREVA, IRSN) and sand bed filters plus metallic pre-filters (IRSN)) and for innovative ones (i.e., acoustic agglomerators (CSIC), high pressure sprays (RSE), electrostatic precipitators (VTT), advanced zeolites (University Lorraine) and combined wet-dry filtration systems (AREVA)). The data analysis and the derivation of correlations allowed to improve existing models and especially to identify the key variables of phenomena that should be taken into account for model upgrade and future developments.

In particular, current pool scrubbing code modelling implicitly assumes low injection rates and hence only two-phase gas-liquid interactions are considered. Complementary studies by PSI, RSE and CIEMAT in the jet injection regime show that a three phase liquid-gas-droplet model is required for accurate estimates of the aerosol removal in this zone.

PSI work on the two-phase flow characteristics during SGTR accidents when the secondary side is flooded has shown the highly dynamic behaviour of the flow under high gas injection velocity resulting in churn-turbulent flow regime. The flow characteristics differ considerably from the description of the hydrodynamics in the existing pool scrubbing codes with much larger gas bubbles and higher gas velocities being found under the SGTR conditions. In particular, the detailed bubble size, shape, interfacial area and velocity data will allow more credible estimates of the multiphase phenomena than corresponding models in low injection regimes. In addition, the confining effect of submerged structures was shown by comparing the distribution of flow using a tube bundle with a bare pool with a single injection tube.

RSE data both on bubble hydrodynamics and aerosol retention has confirmed how in the jet zone (in the injection zone for a bare pool), a three phase liquid-gas-droplet model is required while in the rise zone taking into account two-phase gas-liquid interactions is enough to estimate the retention. The rising velocity of bubble swarms was confirmed as a key parameter that could be upgraded. Tests with different liquid compositions showed that the lower surface tension of the sea water and the water with surfactant resulted in smaller bubble size, and consequently, lower gas rise velocity than in the pure water. This resulted in higher aerosol retention in the sea water and the water with surfactant than in the pure water.

CIEMAT "jet scrubbing" database has resulted to be too scarce for supporting any reliable model, either mechanistic or empirical. Nonetheless, the work done has shown that a good approximation through an empirical approach might be achieved by proposing expressions based on a reduced number of non-dimensional magnitudes. The proposed correlation is far from being mature, but its provisional implementation in system codes might allow getting "acceptable" results in the time intervals of accidental sequences in which jet injection prevails.

The potential of pool scrubbers for the retention of gaseous iodine, including in the middle and long term, was evaluated by experiments performed by AREVA and IRSN.

AREVA Laboratory screening tests regarding organic iodine retention of pool scrubbing systems were performed on the influence of scrubbing liquid composition, of mixing elements and of temperature at the VESPER34 test facility at AREVA GmbH in Erlangen. These qualitative tests showed the retention potential of the pool system and no model/correlation for code development was investigated. AREVA's conclusion is that alternative filtration methods (e.g. dry filtration) are necessary to reach sufficiently high CH_3I retention.

Tests performed in IRSN EPICUR facility were about the effect of the irradiation on volatility of iodine dissolved in an alkaline solution: gas flow rate, temperature and pH are key parameters that influence iodine volatility. In particular, it was confirmed that keeping an alkaline pH in the scrubber solution was absolutely necessary in order to avoid large delayed iodine release. Furthermore, even with alkaline pH, the performance of pool-scrubber type FCVS might be limited by possible HOI volatilization phenomenon. So, in order to avoid an under-estimation of the source term in case of alkaline pH, it is proposed to implement the models developed for HOI transfer and instantaneous conversion into molecular iodine (I_2) in the gaseous phase in ASTEC V2.1.

For sand bed filters, tests in the IRSN EPICUR facility were performed in order to check the stability of caesium iodide (CsI) aerosols trapped on a sand bed filter. CsI aerosols are not stable under temperature (100 to 120 °C) and irradiation and a significant release of I_2 was observed. About half of the inventory is released during 24h as an inorganic gaseous species. A model of CsI radiolytic decomposition was set up and a kinetics equation was optimized. Its order of magnitude is in good agreement with previous optimizations performed in the framework of the OECD-STEM project. No gaseous iodine was released under irradiation from CsI decomposition on a metallic filter. It is believed that gaseous iodine might have been formed by CsI decomposition and then quickly trapped by the metallic filter.

About innovative systems, an experimental system was developed by CSIC and tested in collaboration with CIEMAT using the PECA vessel facility for the acoustic agglomeration at 21 kHz of SiO_2 and TiO_2 particles of 0.3, 1, and 2.5 μm. Results confirmed that agglomeration increases with particle number concentration and size dispersion and is proportional to acoustic intensity and treatment time. For treatment times of about 80 seconds and particle number concentrations in the range of 10^4-10^5 #/cm^3 the smaller particles (0.3 μm) experience a reduction of over 90 % with an acoustic intensity of about 155 dB. A numerical model, based on the fundamental interaction effects between acoustic waves and aerosol particles, was developed in MATLAB code and experimentally validated. Based on the model, the acoustic power required in case of a severe accident could be established (e.g. with aerosols of 0.5 μm, concentration of 0.1 g/m^3 and flow rate of 5 kg/s, about 240 kW are required for a particle number reduction of 90%).

Another innovative system was tested by RSE. It is based on high pressure sprays that can remove at least 99.9 % of suspended 1.5 μm particles in a time of the order of a minute with a single-hole spray nozzle operating at 130 bar. Removal rate depends on spray pressure. The phenomenon on which the aerosol retention is based consists of interaction between droplets generated by sprays and fine particles. Models on droplet-droplet interaction and droplet-aerosol particle interaction were tested: key parameters are droplet and aerosol sizes. The spray removal can be described by a single droplet capture efficiency. The mechanical phenomena involved in the capture are the inertial impaction, interception and Brownian diffusion. The comparison between the model and the experimental data confirms that for aerosol particles smaller than 3 μm, the mechanical phenomenon of interaction between particles and droplets is mainly due to interception and Brownian diffusion, even for small droplets (25-35 μm) and even if, in the model, the inertial impaction for these small droplets is not negligible.

The experimental work carried out at VTT has been devoted to the trapping of iodine species (I_2, CH_3I) in a wet electrostatic precipitator filtration system (WESP). Indeed VTT developed a technique consisting of, in a first step, oxidising gaseous iodine into iodine oxide particles by ozone before entering the WESP. The trends, observed between the specific WESP parameters and the filtration efficiency of gaseous iodine, are valid specifically for the studied range of parameters and for the applied geometry of WESP together with the ozone feed. Evolution of the iodine filtration efficiency according to the number of active corona needles, strength of electrical field, gas flow rate, use of droplets spraying and flushing walls with sodium hydroxide solution, nature and concentration of gaseous iodine and volume fraction of steam in the carrier gas was established. Key phenomena which will have to be taken into account in scaling-up of the facility to real condition were determined.

UniLor and IRSN have performed experimental studies to evaluate the capacity of zeolites to trap molecular iodine and organic iodides in severe accident conditions. Zeolite structure and composition, influence of carrier gas (steam, gas pollutants) and irradiation effects were studied. This study represents a significant improvement in the knowledge of silver zeolites in the context of severe accident. Faujasite Ag/Y, and Ag/X sorbents with more than 15 wt% silver, displayed the highest ability for iodine trapping: both molecular and organic iodine could be trapped with high efficiency and the trapping was irreversible, even under irradiation. It was concluded that the trapping stability depends on the availability of silver sites to promote silver iodide formation. Overall, increase of the silver content in silver-exchanged zeolites improves both the adsorption properties and trapping stability. Nevertheless, a silver content about 9-10 wt% may be enough for severe accident application. Finally, the good behaviour of silver zeolites was checked in conditions close from those anticipated in a severe accident. The only point which should be further studied is the effect of some potential inhibitors in a wider range of conditions than those tested during this study.

The AREVA FCVS PLUS consists of three complementary filtration stages (a high-speed Venturi section, a Metal fiber filter section and a dry sorbent section of zeolites located downstream of an orifice plate which allows passive speed and sliding pressure control including superheating). The focus of the PASSAM study is on the organic iodine retention in the third, newly developed, additional retention stage tested at the large-scale JAVA facility at the technical centre of AREVA GmbH in Karlstein. The tested full scale process sections can be seen as representative for the FCVS and an appropriate design methodology based on empirical correlations had been developed from test results (exact correlations depend on the system used as the type of sorbent material, the geometry of the filtration stage, the flow conditions, etc.). The most important parameters for the retention efficiency to consider for this type of system are superheating of the gas stream and residence time in the sorbent bed.

REFERENCES

1. D. Jacquemain, S. Guentay, S. Basu, M. Sonnenkalb, L. Lebel, H.J. Allelein, B. Liebana Martinez, B. Eckardt and L. Ammirabile, "Status Report on Filtered Containment Venting", *OECD/NEA/CSNI/R(2014)7*.

2. H. J. Allelein, A. Auvinen, J. Ball, S. Guentay, L. E. Herranz, A. Hidaka, A. Jones, M. Kissane, D. Powers and G. Weber, "State-of-the-art on nuclear aerosols", *OECD/NEA/CSNI/R(2009)5, p 248-255*.

3. P. Chatelard, S. Belon, L. Bosland, O. Coindreau, F. Cousin, C. Marchetto, H. Nowack, L. Piar, "Focus on the main modelling features of ASTEC V2.1 major version", 7th *European Review Meeting on Severe Accident Research (ERMSAR 2015), Marseille (France), March 24-26, 2015*.

4. L. E. Herranz, T. Lind, K. Dieschbourg, E. Riera, S. Morandi, P. Rantanen, M. Chebbi and N. Losch, "PASSAM "State-of-the-art report" - Technical Bases for Experimentation on Source Term Mitigation Systems", *PASSAM-THEOR-T04 [D2.1] (2013)*. https://gforge.irsn.fr/gf/project/passam/docman/PUBLIC%20FILES/

5. L. E. Herranz, T. Lind, C. Mun, E. Riera, S. Morandi, P. Rantanen, B. Azambre and N. Losch, "PASSAM Experimental Tests Matrixes", *PASSAM-THEOR-T06 [D2.2], (2014)*, https://gforge.irsn.fr/gf/project/passam/docman/PUBLIC%20FILES/

6. *PASSAM 1st Workshop on source term mitigation of severe accidents, Madrid (Spain), February 26th, 2014*, https://gforge.irsn.fr/gf/project/passam/docman/PUBLIC%20FILES/PASSAM%201st%20Workshop%20Madrid%20Feb%2026,%202014/

7. L. E. Herranz, R. Delgado, T. Berschart, T. Lind and S. Morandi, "Remaining issues on pool scrubbing: Major drivers for experimentation within the EU-PASSAM project", *Proceedings of ICAPP '14, Charlotte, USA, April 6-9, 2014*.

8. A. Dehbi, D. Suckow and S. Guentay, "Aerosol retention in low-subcooling pools under realistic accident conditions", *Nuclear Engineering and Design, Vol. 203, p. 229–241 (2001)*.

9. L. E. Herranz, V. Peyres, J. Polo, M. J. Escudero, M. Espigares and J. López Jiménez, "Experimental and analytical study on Pool Scrubbing under jet injection regime", *Nuclear technology, Vol. 120, p. 95–109 (1997)*.

10. S. Guentay, "ARTIST: introduction and first results", *Nuclear Engineering and Design, Vol. 231, p. 109–120 (2004)*.

11. T. Lind, A. Dehbi and S. Guentay, "Aerosol retention in the flooded steam generator bundle during SGTR". *Nuclear Engineering and Design, Vol. 241, p. 357–365 (2011)*.

12. T. Lind, N. Losch, L. Herranz, C. Mun and S. Morandi, "Advances on understanding of pool scrubbing for FCVS based on the PASSAM project", *IAEA: I3-TM-50122 Technical Meeting on Severe Accident Mitigation, Vienna, 31 August to 3 September 2015*.

13. D. Darmana, N.G. Deen and J. Kuipers, "Parallelization of an Euler–Lagrange model using mixed domain decomposition and a mirror domain technique: Application to dispersed gas–liquid two-phase flow"; *Journal of Computational Physics, Vol. 220, p. 216–248 (2006)*.

14. C. Berna, A. Escrivá, J.L. Muñoz-Cobo and L.E. Herranz, "Enhancement of the SPARC90 code to pool scrubbing events under jet injection regime", *Nuclear Engineering and Design, Vol. 300, p. 563-577 (2016)*.

15. E. Porcheron, P. Lemaitre and D. Marchand, *Aerosol Removal by Emergency Spray in PWR Containment*, *Journal of Energy and Power Engineering, Vol. 5, p. 600-611 (2011)*.

16. A. Del Corno, S. Morandi, A. Cavallari and F. Parozzi, "Experimental report for spray agglomeration system tests", *PASSAM-INNOV-T22 (2017)*.

17. C. Martinez-Bazan, J.L. Montanes and J.C. Lasheras, "On the breakup of an air bubble injected into a fully developed turbulent flow. Part 1. Breakup frequency", *J. Fluid Mech.,* **Vol. 401**, p. 157–182 (1999).

18. W. C. H. Kupferschmidt, J. Ball, J. B. Buttazoni, G. Evans, D. J. Jobe, A. J. Melnyk, A. S. Palson, R. Portman and G. G. Sanipelli, "Final report on the ACE-RTF experiments", *Whiteshell Nuclear Research Establishment, ACE-TR-B3 (1992).*

19. J. Ball, C. A. Chuaqui, J. A. Meritt, R. Portman and G. G. Sanipelli, "Results from PHEBUS RTF2 test: Final report", *COG-95-505, COG-PHEBUS-FP-10, AECL (1998).*

20. J. Ball, C. A. Chuaqui, G. Glowa, J. A. Meritt, R. Portman and G. G. Sanipelli, "Results from PHEBUS RTF6 test: Final report", *COG-97-246, COG-PHEBUS-FP-14, AECL (1998).*

21. B. Clement and B. Simondi-Teisseire, "STEM: An IRSN project on source term evaluation and mitigation", *Transactions of the American Nuclear Society - 2010 ANS Annual Meeting; Las Vegas, NV, U.S.; November 7-11th, 103, 475-476 (2010).*

22. E. Riera, I. González-Gómez, G. Rodriguez and J.A. Gallego-Juárez, *Chapter 34* in *Power Ultrasonics, Cambridge, W P - Elsevier, p. 1023-1058 (2015).*

23. S. Temkin, *Elements of Acoustics. New York: John Wiley & Sons Inc. (1981).*

24. L. Song, G. H. Koopmann and T. L. Hoffmann, "An Improved Theoretical Model of Acoustic agglomeration", *Journal of Vibration and Acoustics*, Vol. 116 (2), p. 208-214 (1994).

25. L. Herranz, T. Lind, K. Dieschbourg, E. Riera, S. Morandi, P. Rantanen, M. Chebbi and N. Losch, *Proceedings of NUTHOS-10, Okinawa, Japan, December 14-18, 2014.*

26. E. Riera, M. Aleixandre, J.A. Gallego-Juãrez, L. Herranz and R. Delgado-Tardáguila, "Experimental report for acoustic agglomeration systems tests", *PASSAM-INNOV-T14 [D4.1] (2016).*

27. D. A. Powers and S. B. Burson, "A Simplified Model of Aerosol Removal by Containment Sprays", *NUREG/CR-5966, SAND92-268 (1993).*

28. C. Riehle, "Applied electrostatic precipitation", Chapter 3, p 25-88, "Basic and theoretical operation of ESP's", *Edited by K.R. PARKER, Chapman & Hall, London, UK (1997).*

29. J. Chang, Y. Dong, Z. Wang, P. Wang, P. Chen and C. Man, "Removal of sulphuric acid aerosol in a wet electrostatic precipitator with single terylene or polypropylene collection electrodes", *Journal of Aerosol Science,* **Vol. 42**, p. 544–554 (2011).

30. T. Kärkelä, J. Holm, A. Auvinen, R. Zilliacus and U. Tapper, "Experimental study on iodine chemistry (EXSI) – Containment experiments with elemental iodine", *VTT Research report VTT-R-00717-09 (2009).*

31. T. Kärkelä, J. Holm, A. Auvinen, R. Zilliacus, T. Kajolinna, U. Tapper, H. Glänneskog and C. Ekberg, "Gas phase reactions of organic iodine in containment conditions", *Proceedings of ICAPP 2010, San Diego, CA, USA, June 13-17, 2010.*

32. A.C. Vikis and R. MacFarlane, "Reaction of Iodine with Ozone in the Gas Phase", *The Journal of Physical Chemistry, Vol. 89, p. 812-815 (1985).*

33. M. Gouëllo, J. Hokkinen, T. Kärkelä and A. Auvinen, "Combination of Ozone Feed and Wet Electrostatic Precipitator: Experimental Study of An Innovative System to Filter Gaseous Iodine and Iodine Containing Particles", *Proceeding of the ICAPP2017 International Congress on Advances in Nuclear Power Plant, Fukui and Kyoto (Japan), April 24-28, 2017.*

34. M. Chebbi, B. Azambre, L. Cantrel and A. Koch, "A combined DRIFTS and DR-UV-Vis spectroscopic operando study on the trapping of CH3I by silver-exchanged faujasite zeolite", *Journal of Physical Chemistry C, Vol. 120, p. 18694-18706(2016).*

35. C. Boulet, M. Miklautsch, N. Losch, P. Zeh and S. Buhlmann, "PASSAM Report WP 4.5 - Experimental report for combined filtration systems", *PASSAM-INNOV-T09 [D4.5] (2015).*

36. A. Del Corno, F. Parozzi, T. Lind, L. Herranz, L. Bosland, C. Dalibart, N. Losch, M. Miklautsch, E. Riera, T. Karkela, M. Gouello, B. Azambre and L. Cantrel, "PASSAM report on analysis of experimental results and development of simplified models and correlations", *PASSAM-THEOR-T26 [D2.3] (2017).*